China Geology 7 (2024) 533−550

China Geology

Journal homepage: http://chinageology.cgs.cn
https://www.sciencedirect.com/journal/china-geology

Geology and mineralization of the Dongping supergiant alkalic-hosted Au-Te deposit (>100 t Au) in Northern Hebei Province, China: A review

Shi-min Zhen[a, b], Da-zhao Wang[c,*], Zhong-jian Zha[d], Hai-jun Bai[e], Jiang Wang[f]

[a] *Development and Research Center of China Geological Survey, Ministry of Natural Resources, Beijing* 100037, *China*
[b] *Technical Guidance Center for Mineral Resources Exploration, Ministry of Natural Resources, Beijing* 100037, *China*
[c] *State Key Laboratory of Nuclear Resources and Environment, East China University of Technology, Nanchang* 330013, *China*
[d] *Institute of Geological Surveying and Mapping Technology of Anhui Province, Hefei* 230022, *China*
[e] *Third Geological Brigade of Hebei Bureau of Geology and Mineral Resources, Zhangjiakou* 075000, *China*
[f] *Ulanqab Real Estate Registration Center, Ulanqab* 012099, *China*

ARTICLE INFO

Article history:
Received 6 September 2023
Received in revised form 11 November 2023
Accepted 19 December 2023
Available online 20 December 2023

Keywords:
Mineralization and alteration
Alkaline intrusion Au deposit
Physicochemical conditions
Metallogenic model
Oxygen fugacity
Sulfur fugacity
Mechanisms of mineral precipitation
Fluid boiling
Fluorine-enriched fluid
Dongping gold deposit
North China Craton
Mineral exploration engineering

ABSTRACT

The Dongping deposit is the largest alkalic-hosted gold deposit in China containing >100 t of Au. This paper presents a new understanding for Dongping ore system, based on the previous studies. The mineralization originally occurred at 400–380 Ma, simultaneous with emplacement of the Shuiquangou alkaline complex, and was overprinted by the hydrothermal activity in the Yanshanian. Isotope compositions of ores indicate metals of the deposit are mainly provided by the Shuiquangou complex. Ore-forming fluids are characterized by increasing oxygen fugacity and decreasing sulfur fugacity, while tellurium fugacity increased in the Stage II-2 and decreased in Stage II-3. These systematic changes are closely related to the processes of mineral precipitation and fluid evolution. Sulfide precipitation from Stage I to Stage II was triggered by fluid boiling, which leads to the precipitation of Pb-Bi-Te, due to decrement of sulfur fugacity. Condensation of gas phase containing high concentration of H_2Te leads to precipitation of Te-Au-Ag minerals and native tellurium. Based on these hypotheses, this paper present a polyphase metallogenic model as follow. During the Devonian, fluids were released from alkaline magmas, which carried ore-forming materials form the surrounding rocks and precipitate the early ores. During the Jurassic-Cretaceous, fluorine-rich fluids exsolved from highly factionated Shangshuiquan granite, which extracted and concentrated Au from the Shuiquangou complex and the Sanggan Group metamorphic rocks, and finally formed the Dongping gold deposit.

©2024 China Geology Editorial Office.

1. Introduction

The North China Craton is one of the oldest cratons in the world (Zhao GC and Zhai MG, 2013; Zhai MG, 2019). It had undergone five major tectonic cycles, including (1) Neoarchean crustal growth and stabilization, (2) Paleoproterozoic rifting-subduction-accretion-collision, (3) Late Paleoproterozoic-Neoproterozoic multistagerifting, (4) Paleozoic orogenesis at the margins of the craton, and (5) Mesozoic lithospheric thinning and decratonization (Zhai MG and Santosh M, 2013). Numerous gold deposits formed along the northern margin of the North China Craton, primarily distributed along the Yinshan-Yanshan belt. From west to east, this belt comprises several mining districts: the Daqingshan (including Hadamengou, Saiyinwusu, and Wachanggou gold deposits), the Zhangjiakou (encompassing Dongping, Xiaoyingpan, Zhongshangou, and Dabaiyang gold deposits) (Figs. 1a – b), the Yanshan (with Jinchangyu and Yuerya gold deposits), the Liaoxi (including Jinchanggouliang and Paishanlou gold deposits), and the Changbaishan mining district (including Jiapigou, Wachangou, and Xiaotongjiapaozi gold deposits) (Deng J and Wang QF, 2016; Hart CJ et al., 2002; Fu C et al., 2022; Xiao CH et al., 2020, 2023). Gold mineralization in these districts occurred at 6 periods, i.e., ca 350 Ma, ca 250 Ma, ca 200 Ma, ca 180 Ma, ca 150 Ma and ca 129 Ma (Zeng QD et al., 2020). These gold deposits are characterized by two and more hydrothermal events..

First author: *E-mail address*: zshimin@mail.cgs.gov.cn (Shi-min Zhen).
* Corresponding author: *E-mail address*: wangdazhao@ecut.edu.cn (Da-zhao Wang).

Literary editor: Li-qiong Jia
doi:10.31035/cg2023097
2096-5192/© 2024 China Geology Editorial Office.

Copyright © 2024 Editorial Office of China Geology. Publishing services by Elsevier B.V. on behalf of KeAi Communications Co. Ltd.
This is an open access article under the CC BY-NC-ND License (http://creativecommons.org/licenses/by-nc-nd/4.0/).

The Zhangjiakou district in northern Hebei Province is located near the northeast Yanshanian magmatic tectonic belt and is an important gold mineralization district, containing more than 100 gold deposits (Figs. 1a–b; Fig. 2). The Dongping gold deposit (>100 t Au), located in the Zhangjiakou district, is the largest alkaline intrusion-related gold deposit in China (Bao ZW et al., 2016; Wang DZ et al., 2019b). Dongping (Cook NJ et al., 2009; Gao S et al., 2017), Cripple Creek and Golden Sunlight in USA (Spry PG et al., 1997), Emperor in Fiji (Pals DW and Spry PG, 2003; Scherbarth NL and Spry PG, 2006), Acupan and Baguio in the Philippines (Cooke DR and McPhail DC, 2001) and Sacarimb in Romania (Cook NJ and Ciobanu CL, 2004) are typical Au-Ag epithermal deposit, related to alkaline and slightly alkaline intrusive volcanic complexes. The deposit geology, isotope composition, fluid inclusions and physicochemical conditions of Dongping gold deposit have been investigated (Bao ZW et al., 2014, 2016; Cisse M et al., 2017; Cook NJ et al., 2009; Fan HR et al., 2001; Fan GH et al., 2021, 2022; Gao S et al., 2015, 2017; Li H et al., 2018, 2022; Li JL and Makovicky E, 2001; Lu DL et al., 1993; Nie FJ, 1998; Wang DZ et al., 2019a, b, c, 2020a; Yang XA et al., 2019; Zhang ZC and Mao JW, 1995). At present, there are still controversies regarding the mineralization epoch, mechanism of mineral precipitation, and metallogenic model of the Dongping gold deposit.

In this paper, we offer a review of previous studies on the Dongping gold deposit and present a new perspective on its genesis. After comprehensive understanding of the tectonic background, regional mineralization regularity, and geological and geochemical characteristics of ore deposits, the aim of this paper is to reveal mechanism for ore deposition and its genetic relationship with magmatic rocks and the metallogenic model. This study is of great significance to understanding the metallogenesis characteristics and ore-forming mechanism of the Dongping gold deposit, and could provide an important guide for further prospecting works in this district.

2. Exploration history of the Dongping gold deposit

The early geological work in the Dongping mining district primarily focused on survey and evaluation of iron ores. In 1972–1973, the Zhangjiakou Comprehensive Geological Team of the Hebei Provincial Geological Bureau conducted a survey and evaluation of metamorphic iron ore within the alkaline complex of Shuiquangou, submitting the survey and evaluation report for Yaowanzi iron ore. In 1976, the 516 Exploration Team of the First Geological Exploration Bureau of the Ministry of Metallurgy conducted a survey and evaluation of metamorphic iron ore in the western part of Yaowanzi and Dongping Nanshan. From 1978 to 1981, the Third Geological Team of the Hebei Provincial Geological Bureau completed a research project titled “Ore-Forming Geological Conditions and Prospecting Direction of Xiaoyingpan Gold Mine”, which suggested that the Shuiquangou alkaline complex was overprinted by strong potassic alteration exhibited characteristics of both magmatic activity and strong multi-stage potassium-dominated mixed rock alteration.

In 1984, the Eighth Brigade of the People’s Armed Police Force (PAP) conducted field survey of the heavy sand anomalies in the district. With 1∶50000 sediment and heavy sand measurements in the region, ten Class A and eight Class B anomalies were identified. In 1985, based on a sample clue provided by a villager, the PAP’s Eighth Brigade discovered a gold-bearing quartz vein, marking the beginning of prospecting for the Dongping gold mine. From 1985 to 2005, the PAP’s Eighth Brigade conducted surveys and explorations of gold mines and developed the “Dongping-type” gold ore-forming model. They successively conducted comprehensive surveys of the Dongping No.1, 2, 3, 22, 26 and 70 vein, and submitted exploration geological reports. In 2006, Zijin Mining Group took over the Dongping gold deposit and furthered exploration work. From 2006 to 2010, detailed surveys of the No.70 and 3 veins were conducted, and detailed survey geological reports for the No.70 and 3 veins were submitted. In 2011, a survey geological report for the deep and marginal parts of the No.70 vein cluster was submitted.

In recent years, the exploration of Dongping Gold Mine has been more concentrated in the deep and edge of existing ore bodies. The mineral resources of Dongping gold mine are facing the risk of depletion, and there is an urgent need for theoretical innovation to guide exploration practice.

3. Regional geology

The Dongping gold deposit is about 10 km south of the Shangyi-Chongli-Chicheng fault (Fig. 1b). The stratigraphic units exposed in the district include the Neoarchean Sanggan Group, Proterozoic Hongqiyingzi Group, Mesoproterozoic Changcheng Group, and Jurassic and Quaternary volcanic sedimentary rocks (Fig. 1b). The Archean Sanggan Group is distributed to the south of the Shangyi-Chongli-Chicheng fault, and is composed of the Xigeyu, Shuidizhuang, Huajiaying, Jiangouhe and Aijiagou formations. The Sanggan Group comprises amphibolite, granulite gneiss, migmatite, marble, with mafic to felsic volcaniclastic and clastic protoliths. The Hongqiyingzi Group is exposed to the north side of the Shangyi-Chongli-Chicheng fault. The Changcheng Group is located in the southeast of this district and consists of marine sedimentary rocks. The Cretaceous Zhangjiakou Formation consists of rhyolite, rhyolite and trachyte, are widely distributed in this district (Fig. 1b).

The Shangyi-Chongli-Chicheng fault is a regional primary fracture in this district, which runs east-west and ends at Shangyi, Chicheng, Chengde and Pingquan, with a total length of 470 km (Fig. 1b). It formed during the Mesoproterozoic, and is a multi-stage fault system from ductile to brittle, which is still an important seismically active zone (Zhang HF, 2007). The Shangyi-Chongli-Chicheng fault controlled the distribution of Proterozoic and Paleozoic

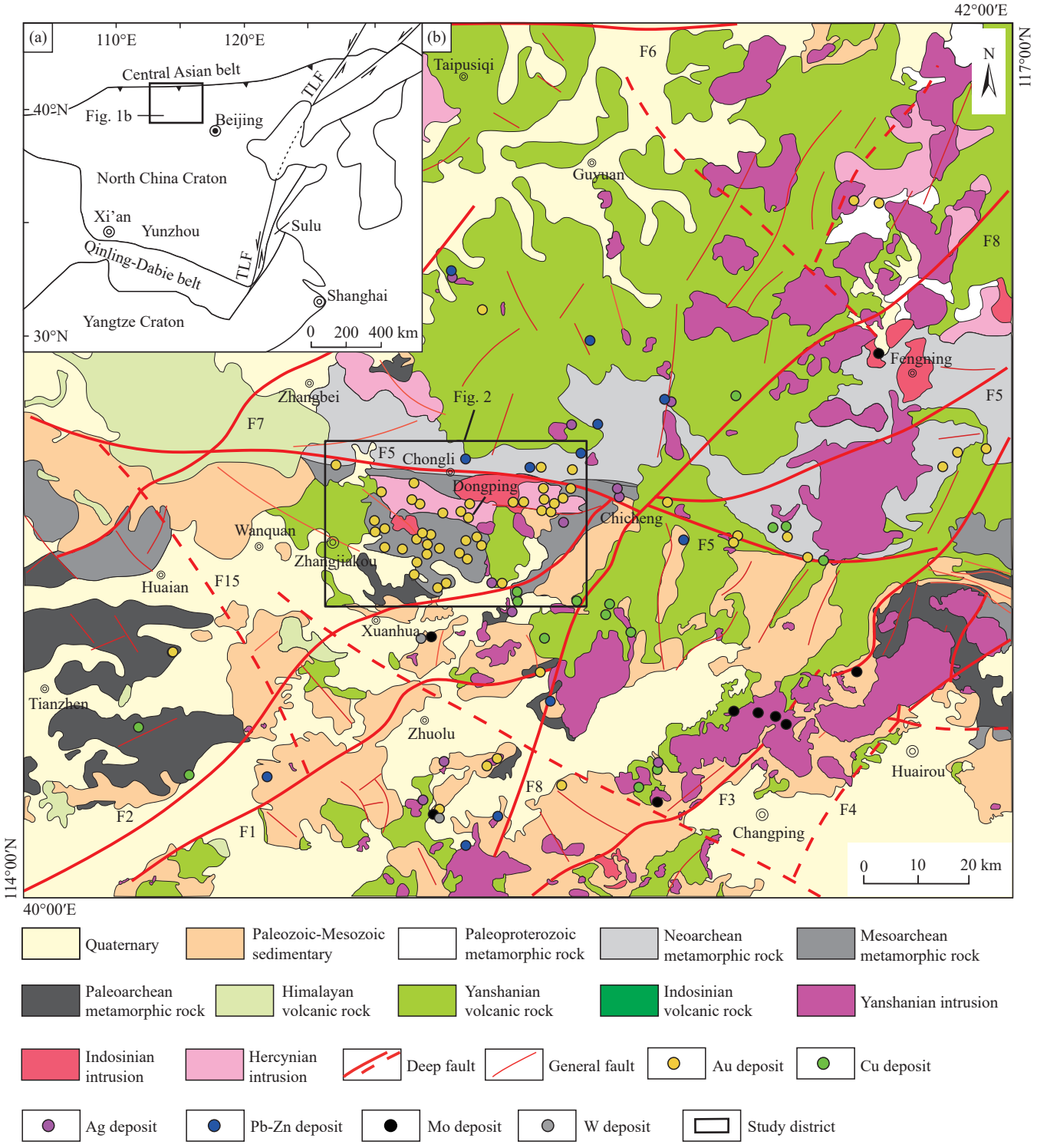

Fig. 1. Sketch maps of (a) geotectonic location and (b) tectonic-magmatic framework of the Zhangjiakou district (modified from Zhen SM et al., 2021). F1-South fault of the Sanggan-Pingquan structure belt; F2-North fault of the Sanggan-Pingquan structure belt; F3-Zijingguan-Lingshan fault; F4-Piedmont fault of the Taihang mountain; F5-Shangyi-Chongli-Chicheng fault; F6-Kangzhuang-Weichang fault; F7-Zhangbei-Guyuan fault; F8-Shanghuangqi-Wulonggou fault; F15-Mashikou-Songzhikou fault.

magmatic rocks and provided favorable structural environment for mineralization. A series of secondary faults developed along the Shangyi-Chongli-Chicheng fault, including (1) the Shangtaizicheng-Wenquan fault, which is about 27 km long and cuts the Shuiquangou complex, Xiaozhangjiakou ultrabasic rock and Wenquan granite; (2) the Xisanjianfang-Womakeng fault, about 45 km long and parallel to Shangtaizicheng-Wenquan fault, which cuts the Shuiquangou complex and Xiaozhangjiakou ultramafic rock; (3) the Hanjiagou-Guzuizi-Changdi fault, about 30 km long and strikes NW-SE, which cuts through the volcanic rocks of the Zhangjiakou Formation and Shuiquangou complex (Zhen

SM et al., 2021).

A number of intrusive complex are distributed in the Zhangjiakou district, including the Devonian Shuiquangou alkaline complex (Miao LC et al., 2002; Li CJ et al., 2012; Zhen SM et al., 2021), the Triassic Guzuizi, Honghualiang and Xiangshuigou granites (Jiang N et al., 2007; Miao LC et al., 2002), the Xiaozhangjiakou ultramafic rocks (Tian W et al., 2007), and the Cretaceous Shangshuiquan, Beizhazi, and Zhuanzhilian granitoids (Miao LC et al., 2002; Jiang N et al., 2009). Distributions of intrusions are controlled by the Chongli-Chicheng fault and show east-west trend, while magmatic activities during the Yanshanian appear to be controlled by the northeast Yanshanian magmatic structural zone (Fig. 1b).

The Devonian Shuiquangou complex intruded metamorphic rocks of the Sanggan Group. The EW-trending intrusive complex is ca. 55 km long, 5–8 km wide, with exposed area of ca 350 km^2 (Miao LC et al., 2002). The western part of the complex is mainly composed of augite/hornblende syenite, and the middle part contains augite/aegirine syenite. The eastern part is more felsic, and comprises mainly syenite and quartz syenite. No clear boundaries exist among these lithologies, and most of them show gradational contact. The complex was intruded by the Honghualiang, Wenquan and Shangshuiquan intrusions and overlain by the Zhangjiakou Formation volcanic rocks. Emplacement ages of the complex range from 400 Ma to 373 Ma, showing an eastward younger trend (Miao LC et al., 2002; Zhen SM et al., 2021). Jiang N (2005) argued that the complex was mainly derived from the enriched lithospheric mantle, and reflects a post-collision extensional regime after the arc-continent collision between the Bainaimiao island arc and the NCC.

The Triassic Guzuizi, Honghualiang and Xiangshuigou granites are indistinguishable in emplacement ages, mineral and chemical compositions, indicating that they may represent different outcrops of a batholith. These Triassic granites were emplaced at 236–231 Ma (Miao LC et al., 2002; Jiang N et al., 2007) and are adakite-like, which is interpreted to have formed by partial melting of ancient lower crust upon mantle upwelling (Zhen SM et al., 2021).

The Shangshuiquan granite is located southeast of the Dongping gold deposit. The granites intruded the Shuiquangou syenite complex and the Sanggan Group, and was overlain by volcanic rocks of the Zhangjiakou Formation. The Shangshuiquan granite (ca 140 Ma) is highly evolved, and was likely derived from partial melting of the ancient lower crust (Jiang N et al., 2009).

A porphyritic granite intrusion was recently discovered in the Zhuanzhilian section of the Dongping gold deposit (Fig. 3), which is consistent with geophysical inference of deep rock masses (Zhen SM et al., 2019). There is as many as one tonnage of Au in the fractured shear zone within the porphyritic granite intrusion. Using the zircon U-Pb dating, Wei H et al. (2018) believe that the main gold mineralization occurred at 142.06 ± 0.84 Ma.

Ore deposits in the northern margin of the North China Craton exhibit characteristics of concentrated spatial distribution. The ore zones exhibit an equidistant distribution pattern, with a pronounced concentration of polymetallic mineralization occurring at the intersection of the east-west and NEE (northeast to east) ore zones (Cui SQ et al., 2002). The Zhangjiakou district is rich in mineral resources and contains a large number of Au deposits (such as Dongping, Xiaoyingpan, Zhongshanguou and Zhangquanzhuang deposits), Pb-Zn deposits (such as Caijiaying, Sanyizhuang and Sandaogou deposits) and Ag deposits (such as Pengjiagou, Sunjiazhuang and Jinjiazhuang deposits), and a small number of Cu deposits (Xiangshan Cu deposit) and Mo deposits (Zhangmajing and Jiajiaying Mo deposits) (Fig. 1b). Gold deposits are primarily concentrated within the intersecting segments of near-east-west faults and the nearby north-south, northeast, and northwest fault structures.

4. Deposit geology

The Dongping gold deposit is located in the Zhangjiakou district at the northern margin of the North China Craton. The strata exposed in the mining district are mainly the Jiangouhe Formation of the Archean Sanggan Group (Fig. 2). The lithology comprises mainly amphibolite gneiss, amphibolite, biotite schist and leptite, and the primary rock is intermediate-basic volcanic rock (Wang DZ et al., 2019b).

Gold mineralization is controlled spatially by three-stage faults (Bao ZW et al., 2016; Song GR and Zhao ZH, 1996). The first-stage faults are filled by barren or weakly gold-mineralized quartz veins. The second stage faults are the main gold-controlling structure (Fig. 2). The orebodies are characterized by subparallel NNE-striking auriferous quartz-K-feldspar veins (Fig. 3; Li SZ and Qi GC, 2000). The third stage faults were observed locally, comprising NE-trending tensional shear faults. Gold mineralization associated with the third-stage faults is minor and restricted to the western part of the ore field (Li HY et al., 2000).

The igneous rocks exposed within the deposit area predominantly comprise Shuiquangou syenite, together with numerous intrusive dikes, including pegmatite and granite porphyry dikes (Fig. 3). Notably, the primary structural framework governing the presence and spatial distribution of these magmatic rocks and associated ore deposits within the mining area is the Shangyi-Chongli-Chicheng fault, characterized as a first-order structural feature (Jiang SH and Nie FJ, 2000; Li HY et al., 2000). Supplementary to this primary fault structure, secondary fault systems play a key role in controlling the localization of ore veins within the Dongping gold deposit. These secondary faults encompass the Yangmuwa-Mazhangzi-Jinjiazhuang and Zhongshangou-Honghualiang-Shangshuiquan fault networks (Zhen SM et al., 2021).

5. Alteration and mineralization

5.1. Alteration

The Dongping gold deposit exhibits extensive

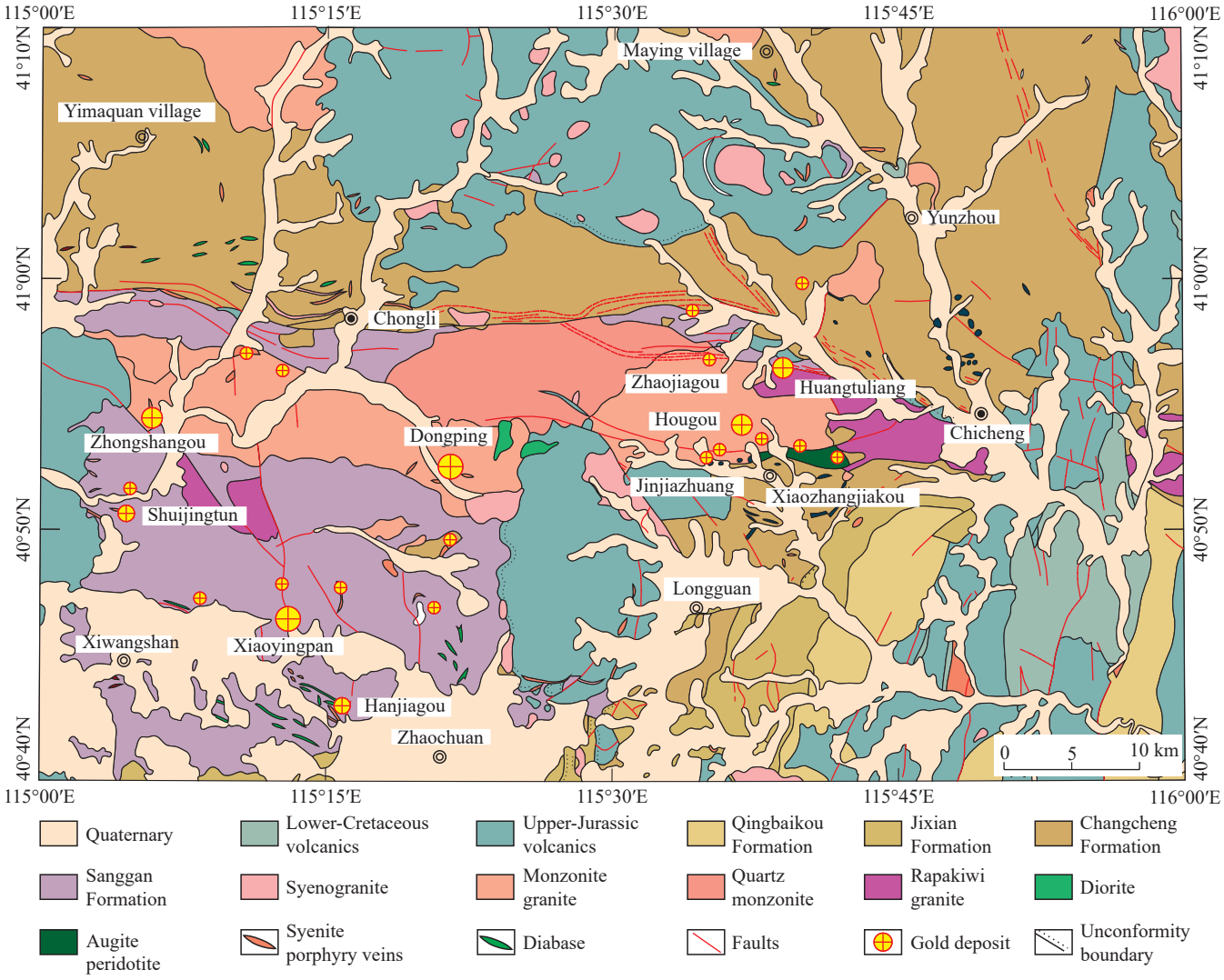

Fig. 2. Sketch map of geology and ore deposits of the Zhangjiakou district (revised from Wang DZ et al., 2019a, 2019b, 2019c).

hydrothermal alteration, including potassic alteration, silicification, chloritization, epidotization and carbonatization (Fig. 4). Among these alterations, potassic alteration prevails as the most widespread. Flaky specularite aggregates are found commonly within areas subjected to potassic alteration. Additionally, gold-bearing quartz-sulfide veins often intersect the K-feldspar veins, signifying that gold deposition postdated potassic alteration. Sericite typically replaced preexisting hydrothermal feldspar and can be observed as fine-grained aggregates. Carbonatization, on the other hand, remains relatively weak and does not display any discernible connection with gold deposition. Late-stage quartz-calcite veins generally cut across the gold-bearing quartz-sulfide veins and are characterized by a deficiency in sulfides.

Gao S et al. (2017) elucidated that, during the process of potassic alteration, there is an enrichment of K_2O, Na_2O, and SiO_2, while TiO_2, Fe_2O_3(tot), MgO, CaO, P_2O_5, and MnO are depleted. There is a significant increase in SiO_2 content, coupled with a depletion of TiO_2, Fe_2O_3(tot), MgO, CaO, and $P_2O_5$when silicification occurred.

5.2. Mineralization

5.2.1. Orebody feature

At present, 69 gold-bearing veins were identified, and these veins are enveloped by the Shuiquangou syenite. Among them, No. 1 and No. 70 stand as the largest gold-bearing veins within the mining area, together comprising 80% of the total gold reserves. The average gold (Au) grade of the ores is 6 g/t, with individual ore bodies ranging from 4 g/t to 23 g/t. Each ore body stretches between 200 m to 400 m in length, with a thickness of 0.12 m to 36 m and extending to depths of 100 m to 600 m. Notably, the density of ore vein increases with depth, with disseminated ores surrounding the veins gradually becoming the majority of ore type at greater depths.

The No. 1 ore body is situated a few hundred meters north of the village of Dongping. It comprises nine gold-bearing quartz veins with varying orientations (NE, NW, and N-S) and dips of 40° to 50° NW. These veins are situated within the monzonite and typically measure between 45 m to 600 m along strike, up to 228 meters along dip, and are 0.5 m to 3 m wide. The ore grades of these veins range from 8 g/t to 23 g/t

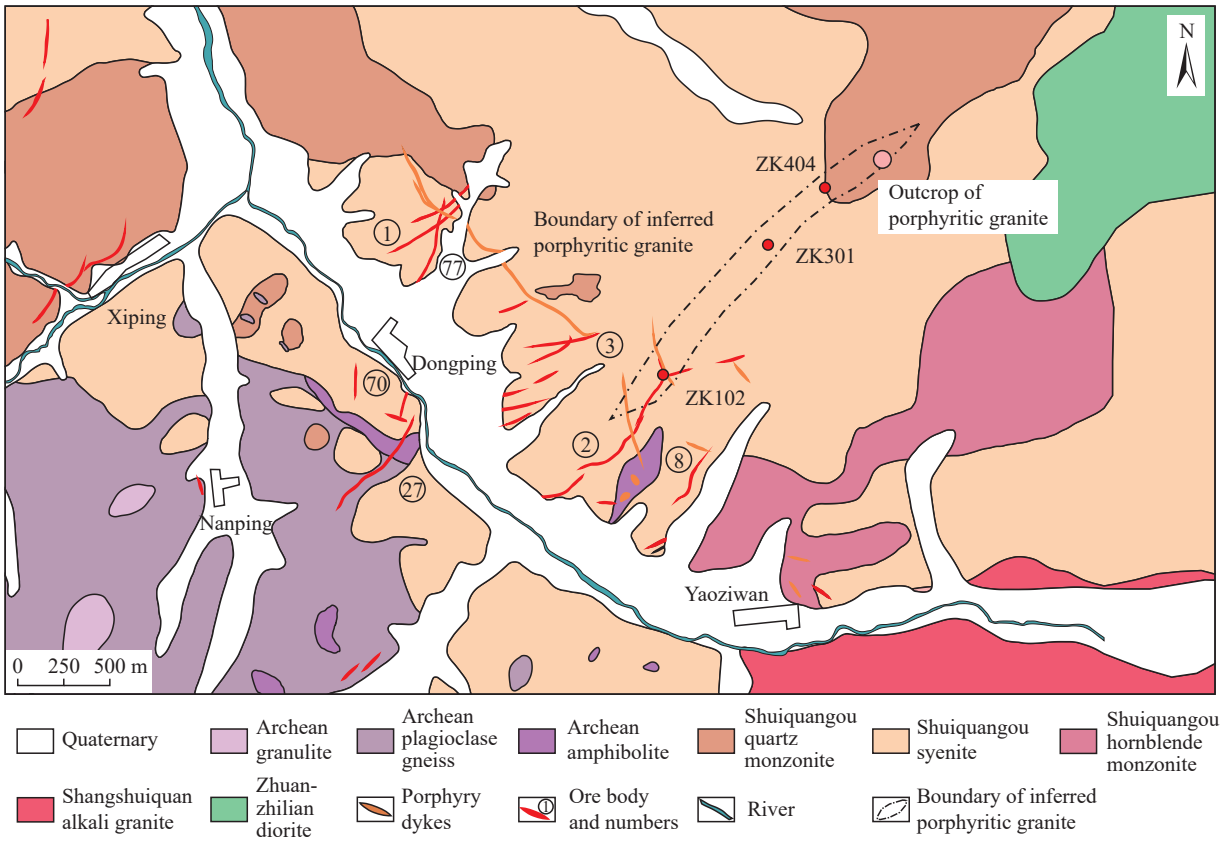

Fig. 3. Geological map of the Dongping gold deposit (modified from Wei H et al., 2018; Wang DZ et al., 2019a, 2019b, 2019c).

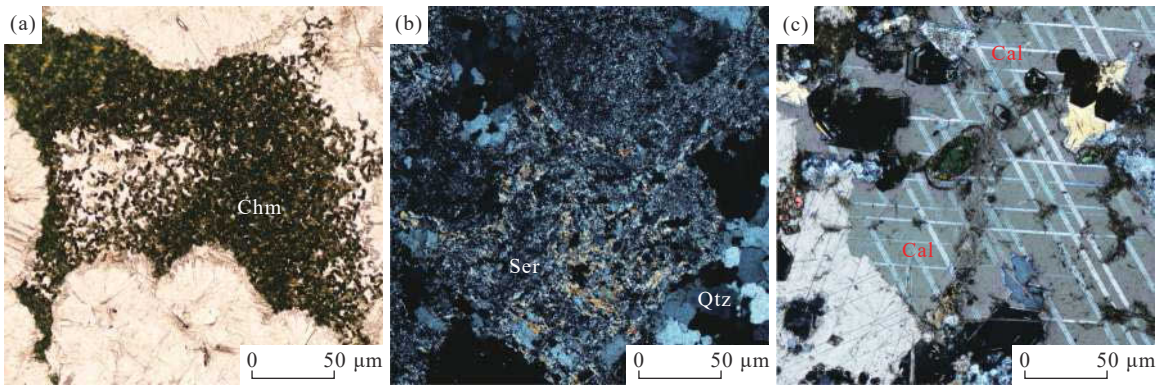

Fig. 4. Photomicrographs of alteration from the Dongping deposit. a–Chloritization; b–sericite; c–carbonatization. Cal –calcite; Chm–chamosite; Qtz–quartz; Ser–sericite.

Au. The veins are characterized by relatively narrow selvages of altered K-feldspar and sulfidized monzonite, which contain disseminated gold. Thinner quartz veinlets, with grades of 2 g/t to 4 g/t Au, occur within secondary fractures in the center of these altered areas. Fracturing along the margins of the veins led to the incorporation of irregular lenses of sheared sulfide-bearing quartz into the immediate wall rocks. The No. 1 vein is fault-controlled, and is brecciated. The resultant breccia contains syenite fragments, ranging in size from several centimeters to several tens of centimeters.

The No. 70 vein continues along strike with the No. 1 ore body and displays large variations in ore grades with changes in elevation (Fig. 5). The No. 70 vein consists mainly of numerous quartz veins with varying lengths, cavities, and breccia of different sizes and irregular shapes. These veins strike at approximately 290–340° NW and dip SW (Fig. 5). All gold ore bodies are hosted within K-altered syenite. These ore bodies have thicknesses ranging from 0.69 m to 1.93 m, with an average thickness of 1.13 m. The gold grades of these ores vary from 1.42 g/t to 43.10 g/t.

The orebodies at Dongping are largely controlled by the fault structures, with the characteristic of an echelon distribution (Zheng YD et al., 1990; Li SZ, 1999; Li SZ et al., 2000). The orebodies are controlled by NNE-trending sinistral and NW-trending dextral echelon structures. Controls of fault structures on the ore distributions, especially the combination are obvious, mainly controlled by the combination of NNE leftward and NW rightward echelon veins(Li SZ, 1999). The

NNE and NW conjugate fault structures belong to shear structures and are the main ore-controlling structures. There is a clear boundary between the NNE ore vein and the surrounding rock, with common traces of compression and sliding, displaying compressive and torsional characteristics. In the NW oriented ore vein zone, every fine vein body is almost thick in the middle and pointed out on both sides, showing extensional and torsional characteristics (Zhen SM et al., 2019).

5.2.2. Ore type

The ore types in the deposit mainly include gold-bearing quartz veins and disseminated ores (Fig. 6), and the disseminated ores increase in density as depth increases, while veins become tainted and gradually replaced by impregnated ores. The thin veins are linear and conjugated and cut off by later fractures.

The ore contains 3%–5% sulfides, which comprise mainly pyrite, galena, sphalerite and chalcopyrite. Quartz veins invaded Archean metamorphic rocks, and large amounts of sulfides were concentrated in and near the contact. Quartz and pyrite are the main host minerals for gold. Magnetite and hematite also were observed in ores (Fig. 6c), which are also typical gold-bearing minerals.

5.2.3. Mineral composition

Minerals in the Dongping gold deposit can be grouped into five categories: Native element mineral, sulfides, tellurides, oxides and oxy-salt mineral (Fig. 7; Wang DZ et al., 2019b).

(i) Native element minerals

Native element minerals in the Dongping gold deposit are mainly native tellurium and native gold. Native tellurium mainly occurs in sulfide-quartz vein, and native gold occurs in magnetite-hematite vein, sulfide-quartz vein and oxidized ore.

Native tellurium: This mineral is characterized by bright white under the reflected light, and the oxidized native tellurium is brown. Native tellurium is mainly distributed along the boundaries of pyrite, and show wormlike texture in pyrite pores. Electron microprobe analyses show that native tellurium has a small amount of S.

Native gold: Native gold grains have sizes of 1–150 μm (Fig. 7a). Native gold in the Dongping gold deposit formed in at least three stages: The earliest native gold mainly occurs as

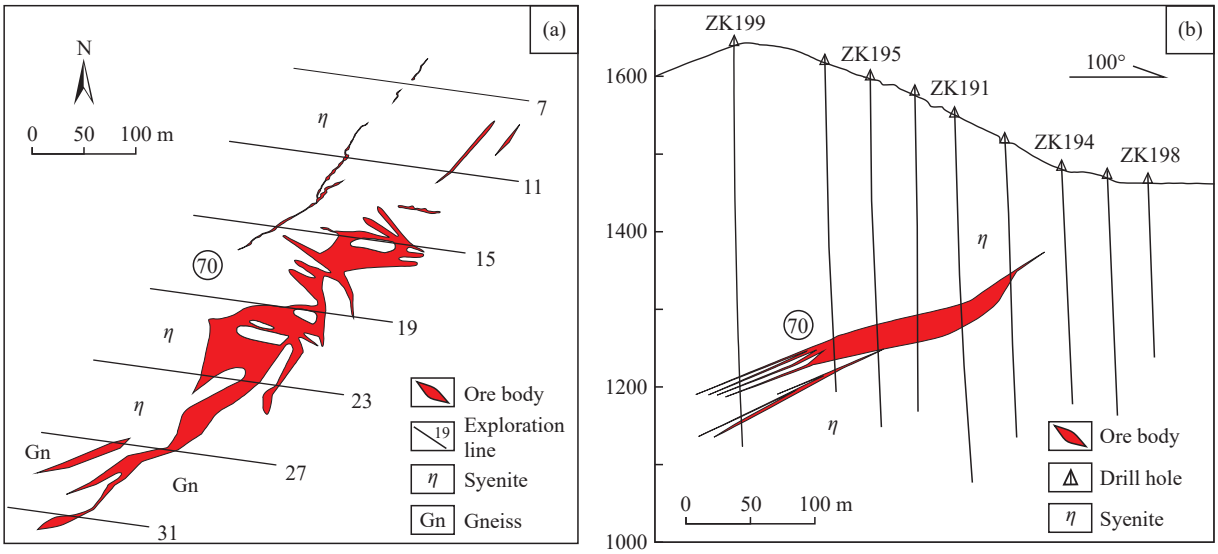

Fig. 5. Horizontal projection (a) and longitudinal sections (b) of No. 70 vein of the Dongping gold deposit (modified from Wang DZ et al., 2019a, 2019b, 2019c).

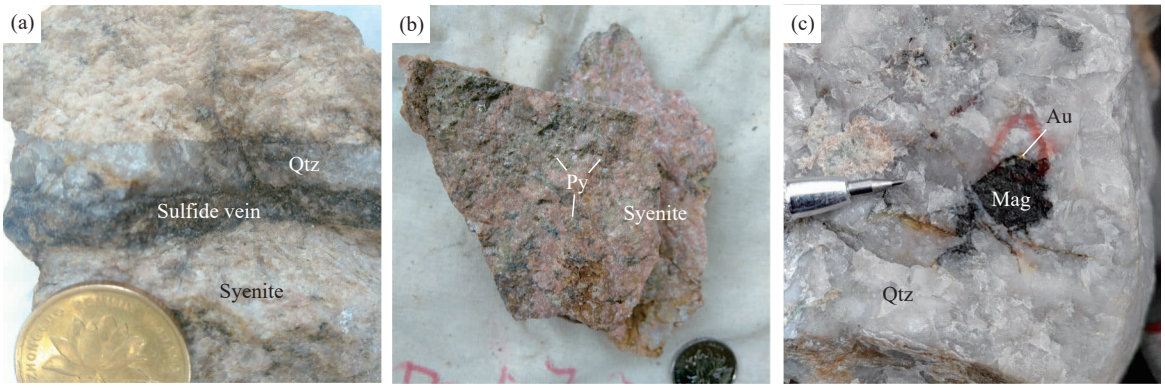

Fig. 6. Photographs of different ore types. a–Auriferous quartz vein; b–disseminated ore; c–oxidized ore. Au–gold; Mag–magnetite; Py–pyrite; Qtz–quartz.

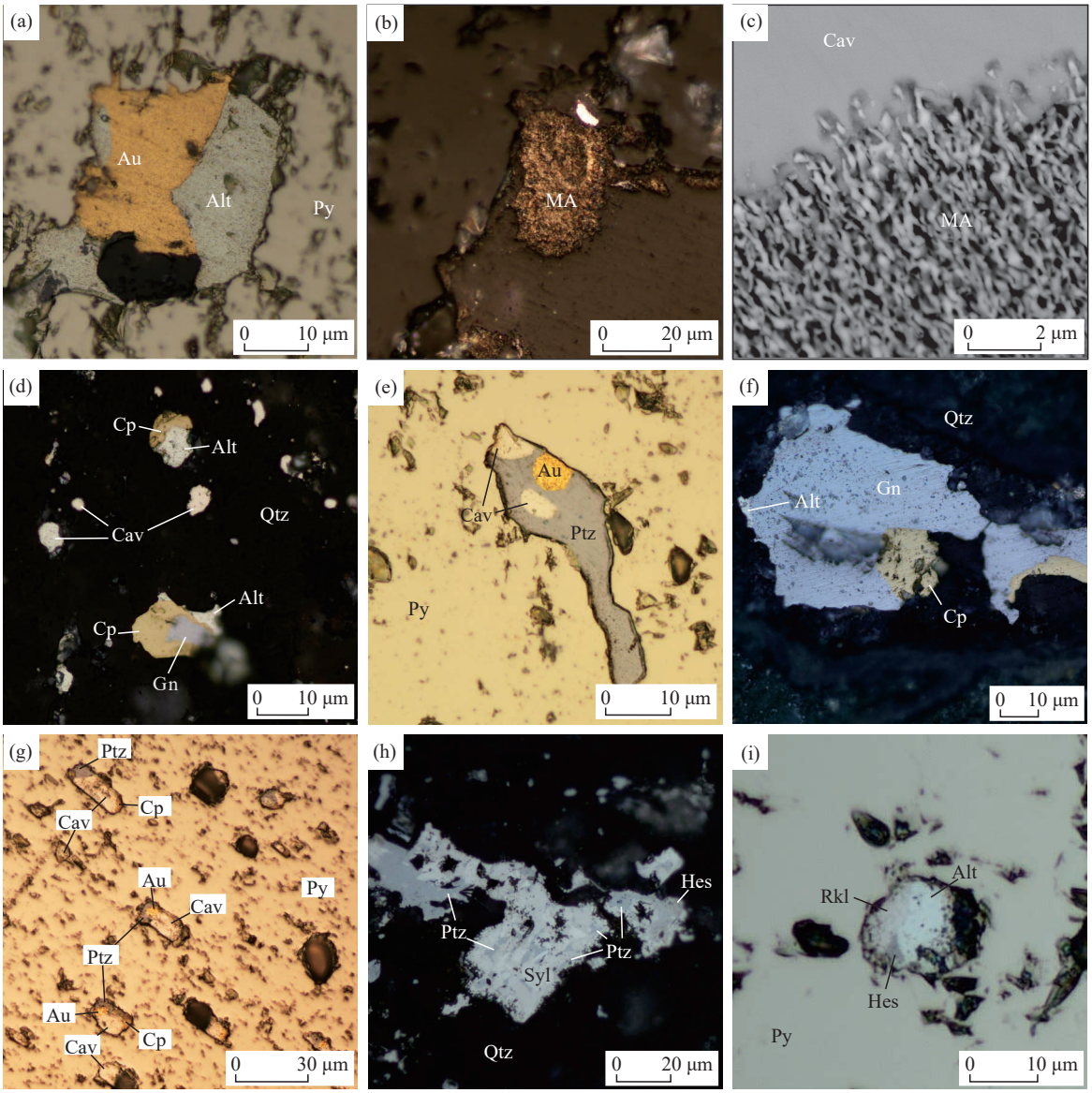

Fig. 7. Photomicrographs of sulfide and telluride mineralization from the Dongping gold deposit. Au–gold; Alt–altaite, Cav–calaverite; Cp–chalcopyrite; Gn–galena; Hes–hessite; MA–microporous gold; Ptz–petzite; Py–pyrite; Qtz–quartz; Rkl–rucklidgeite; Syl–sylvanite.

native gold grains with sizes of 20–150 μm, which was covered by pyrite of the early stage and was replaced by sulfide and telluride of the later stage; in the middle stage, native gold mainly occurs with telluride, with grain sizes of 3–15 μm; in the late stage, native gold is micro-porous, called the microporous gold, which formed by oxidation and alteration of Te-Au-Ag minerals.

Microporous gold is widely distributed in primary and oxidized ores, and often occurs with telluride in quartz or in pyrite as mineral inclusions (Figs. 7b–c). Microporous gold is brownish yellow under reflected light. Scanning electron microscope shows that it has high porosity and is filament-like or worm-like. The microporous gold shares the same shape with the original telluride with grain sizes around 10–80 μm. The maximum pore size in micro-porous gold is 500 nm, and the length of a single native gold crystal is about 0.5–3 μm. However, telluride in oxidized ore is completely dissolved and decomposed. It is generally believed that microporous gold is formed by the decomposition of gold-bearing telluride. During the decomposition of Au-bearing tellurides, Te is dissolved and migrated with the fluid, and finally precipitated as secondary telluride. The contact relationships between microporous gold and residual telluride are complicated, which may be the result of various physical and chemical conditions of hydrothermal fluid and complex nucleation and growth process of the microporous gold.

(ii) Sulfide minerals

Sulfides include pyrite, chalcopyrite, galena, sphalerite and a small amount of molybdenite and bornite.

Pyrite is the most important metallic mineral in the deposit. In the early stage of mineralization (Figs. 7a, 7e, 7g, 7i), pyrite occurs in quartz vein as coarse anhedral grains or in magnetite-hematite vein as anhedral grains. The magnetite-hematite vein in the early stage was cut by the pyrite vein of late stage. Pyrite at Dongping is arsenic-free. Gold content in pyrite can reach 1% in volume (Cook NJ et al., 2009).

Chalcopyrite mainly occurs in magnetite-hematite and sulfide quartz vein as aggregates and inclusions (Figs. 7d, 7f). It is usually associated with tellurium, gold and silver minerals, or occurs as emulsion texture in sphalerite. Galena mainly occurs in pyrite or quartz as aggregates or inclusions, and usually coexists with chalcopyrite, sphalerite and telluride (Figs. 7d, 7f). Sphalerite occurs with chalcopyrite and galena, mainly in magnetite-hematite veins. Sphalerite contains a large number of chalcopyrite inclusions. Molybdenite is rare in ores. It occurs as thin veins or aggregates in pyrite and quartz. Trace amounts of native gold are hosted in molybdenite fractures or inside, indicating that molybdenite formed before or at the same time as natural gold ore formation. Bornite is brown in reflected light, and is associated with chalcopyrite in quartz.

(iii) Telluride minerals

The Dongping gold deposit contains a large amount of tellurides, which occurs in pyrite and quartz as inclusions or as veinlets. Tellurides in the deposit include calaverite, altaite, petzite, sylvanite, hessite, krennerite, stützite, tellurobismuthite, tetradymite and muthmannite, rucklidgeite and volynskite (Fig. 7; Gao S et al., 2015; Wang DZ et al., 2019b; Zhang PH et al., 2002).

Altaite is one of the telluride-richest minerals in the deposit. Altaite and various minerals, such as galena, chalcopyrite, gold, galena and tellurobismuthite, occur in isolated or clustered form (Figs. 7a, 7d, 7f, 7i). The size of individual particles is between 5–50 μm. Calaverite is the most important gold-containing telluride in abundance. It is mainly found in calaverite + gold ± petzite ± chalcopyrite assemblages (Figs. 7c, 7e, 7g). The calaverite + gold assemblage is found in magnetite-hematite. Due to the random distribution of silver at gold sites, calaverite usually contains small amounts of silver (Bindi L et al., 2009). Hessite is light brown or blue in reflected light and has obvious anisotropy (Figs. 7h–i). Petzite is widely distributed and is one of the most important telluride minerals in abundance in this study. Petzite is mainly found in the calaverite + gold + petzite ± chalcopyrite assemblages (Figs. 7e, 7g, 7h). Tellurobismuthite often coexists with gold. Compared to altaite, it shows white to light pink and is brighter than tetradymite in reflected light.

6. Mineralization timing

According to field survey and observation under microscope, three paragenetic stages for the mineralization are suggested in this study (Fig. 8).

Stage I is characterized by K-feldspar quartz veins and magnetite-hematite veins, cut by late sulfide-containing quartz veins. Stage I vein contains potassium-bearing feldspar, magnetite, hematite and pyrite.

Stage II is dominated by telluride and polymetallic sulfide-quartz veins. Polymetallic sulfides are hosted in veins and comprise pyrite, chalcopyrite, galena, sphalerite and molybdenite. Stage II is an important stage of telluride and gold mineralization. Sulfides are occasionally precipitated in the cracks of early quartz veins. Sulfides mainly formed in the early stage, Pb-Bi-Te minerals mainly in the middle stage, and Au-Ag-Te minerals mainly in the late stage.

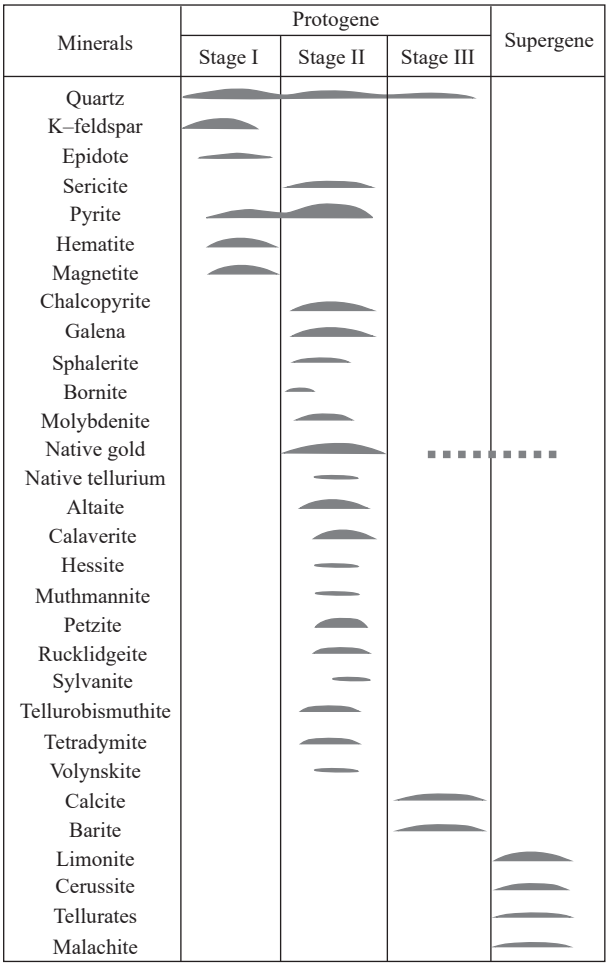

Fig. 8. Paragenetic sequence of minerals in the Dongping gold deposit (modified from Wang DZ et al., 2019a, 2019b, 2019c).

Stage III consists mainly of grey chalcedony-like quartz and a small amount of pyrite. Calcite usually comes in the form of fine veins. No significant gold mineralization was observed at this stage.

7. Discussion

7.1. Geochronology

A large number of geochronological studies have been carried out on the Dongping gold mineralization, but the obtained ages are very scattered, ranging from 380 Ma to 120 Ma (Fig. 9), leading to contradictory explanations of the deposit genesis.

Some researchers have conducted studies on the ^{40}Ar-^{39}Ar ages of hydrothermal K-feldspar and mica collected from the deposit, yielding ore-forming age estimates ranging from 150 Ma to 190 Ma (Hart CJ et al., 2002; Jiang SH and Nie FJ, 2000; Song GR and Zhao ZH, 1996). The ages suggest a hydrothermal event during the Jurassic. However, it is important to note that K-feldspar and mica have low closure temperatures for the ^{40}Ar-^{39}Ar system, and the Ar could be

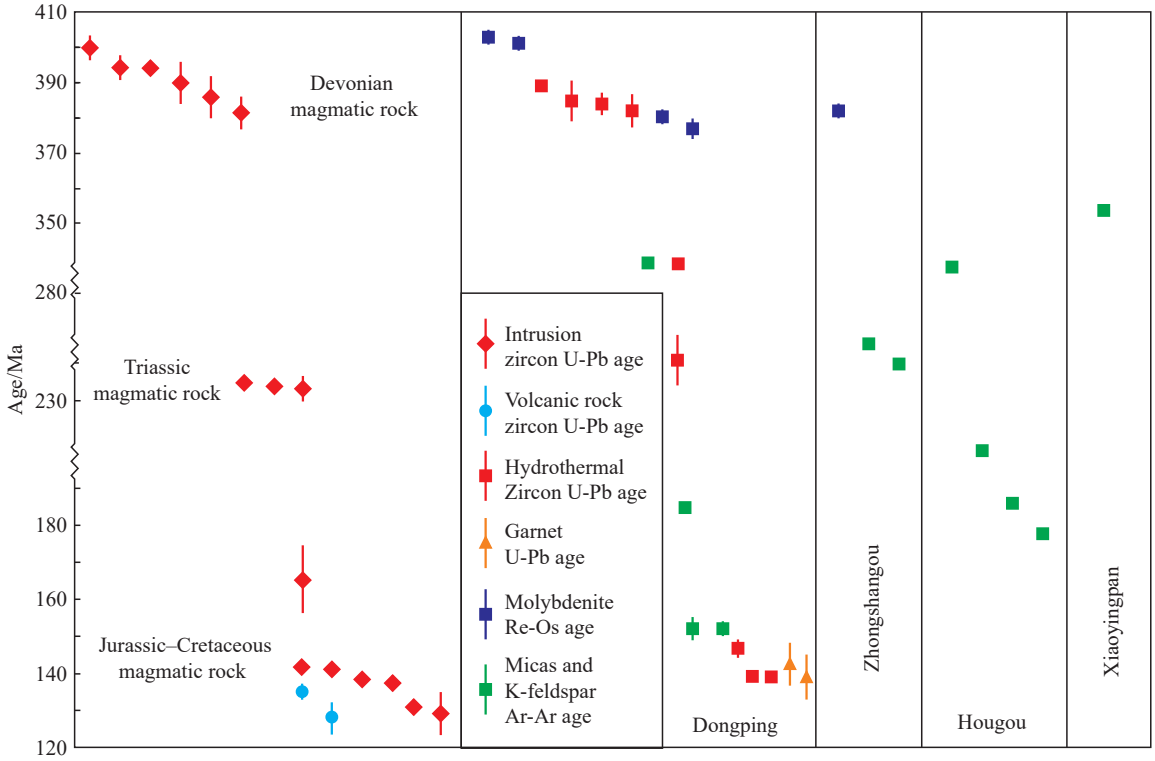

Fig. 9. Distribution diagram of diagenetic and metallogenic ages in the Zhangjiakou district. Diagenetic age source from Miao LC et al. (2002), Yang JH et al. (2006), Jiang N et al. (2007, 2009), Li CJ and Bao ZW (2012), Cisse M et al. (2017) and this paper; metallogenic age source from Wang ZK et al. (1992), Wang DZ et al. (2019b, 2020a), Jiang SH and Nie FJ (2000), Hart CJ et al. (2002), Bao ZW et al. (2014), Li H et al. (2018), Fan GH et al. (2021).

lost or gained during multistage hydrothermal activities (Villa IM and Hanchar JM, 2013), potentially leading to geologically unreliable ^{40}Ar-^{39}Ar ages. In contrast, Bao ZW et al. (2014) and Li H et al. (2018) reported the presence of hydrothermal zircons with ages around 140 Ma ago, suggesting a reliable timing of mineralization. Sample D-19 in Bao ZW et al. (2014) was collected from a quartz vein at the 1184 m level of the No. 1-70 vein system, and contains two period zircons of ca 240 Ma and ca 140 Ma. Wei H et al. (2018) found the gold-bearing porphyritic granite has zircon U-Pb ages of 373.0 ± 3.5 Ma and 142.02 ± 1.2 Ma, indicating a Cretaceous gold mineralization event at Dongping. Additionally, Wang DZ et al. (2020b) obtained Re-Os ages for molybdenite samples from the Dongping deposit, proposing that the ca 400 Ma molybdenite represents the initial mineralization phase and the precipitation of early-stage sulfides. Recently, Fan GH et al. (2021) reported a hydrothermal garnet U-Pb age of approximately 140 Ma from the Dongping deposit, suggesting its association with a Cretaceous gold mineralization event. This hydrothermal garnet is believed to have precipitated from magmatic-hydrothermal fluid sourced from the Early Cretaceous Shangshuiquan granite (Fan GH et al., 2021, 2022).

We argued the Dongping gold deposit is a result of multi-stage hydrothermal systems. Gold mineralization of early stage is closely linked to the emplacement of the Devonian Shuiquangou syenite, which occurred within the timeframe of 400 Ma to 373 Ma (Bao ZW et al., 2014; Miao LC et al., 2002; Zhen SM et al., 2021). In contrast, gold mineralization of late stage is associated with the emplacement of the Cretaceous granite and the subsequent leaching of gold from Archean metamorphic rocks (Li H et al., 2022). It is worth noting that the Devonian Shuiquangou syenite may have played a similar role to that of the metamorphic rocks within the Sanggan Group, serving as a potential source of gold for the mineralization process (Zhen SM et al., 2021). The distribution of gold deposits appears to be controlled by the northeast-oriented Yanshanian magmatic zone and the east-west distribution patterns of the Devonian syenite and the Archean metamorphic rocks. This observation further supports the notion of multi-stage hydrothermal systems as a significant factor in the formation of these deposits (Fig. 1b). Meanwhile, ore-hosting porphyritic granite intrusion, discovered in the Zhuanzhilian section of the Dongping gold deposit, indicates the main mineralization process related to Mesozoic magmatism activities (Wei H et al., 2018). In summary, the tectonic-hydrothermal fluids genetically associated with the Mesozoic magmatism activities may be one of the key factor for the gold mineralization.

7.2. Fluid and material sources

(i) Fluid characteristic

Quartz in this deposit contains three types of fluid inclusions: vapor-rich, liquid-rich, and polyphase. Homogenization temperatures of fluid inclusions within quartz from different stages indicate that the ore-forming

temperature remained relatively stable from Stage I to Stage II. However, there are notable differences in the fluid inclusion types and salinities of fluids. In Stage I, gas-liquid two-phase inclusions predominate, while Stage II has more gas-rich inclusions and liquid CO_2-containing three-phase fluid inclusions, with gas-liquid two-phase inclusions accounting for only 30%. Few fluid inclusions containing halite crystals are observed in Stage II, with salinity ranging from 36.9% to 38.6% NaCl equivalent (Wang DZ et al., 2019b). The transition from Stage I to Stage II is characterized by an increasing proportion of the gas phase and differentiation in salinity, suggesting the occurrence of fluid boiling (Roedder E, 1984). Fluid boiling caused changes in physical and chemical conditions of the fluid, including oxygen fugacity, sulfur fugacity, tellurium fugacity, and pH, leading to the rapid precipitation of minerals (Cooke DR and McPhail DC, 2001). This may explain the precipitation of sulfides and tellurides in Stage II. In Stage III, fluid inclusions have lower homogenization temperatures and Cl^-/SO_4^{2-} ratios compared to those of Stages I and II, indicating an increase in oxygen fugacity of the ore-forming fluid, possibly due to the addition of atmospheric water (Wang DZ et al., 2021). This increase in oxygen fugacity led to the precipitation of minerals such as calcite and barite (Wang DZ et al., 2019b).

The δD and $\delta^{18}O_{H2O}$ values for Stage I range from −97.9‰ to −90.6‰ and 4.9‰ to 5.8‰, respectively. For Stage II, the δD and $\delta^{18}O_{H2O}$ values range from −94.2‰ to −93.2‰ and 5.4‰ to 5.6‰, respectively. Finally, for Stage III, the δD and $\delta^{18}O_{H2O}$ values range from −99.4‰ to −89.8‰ and 0.2‰ to 0.9‰, respectively (Fig. 10a; Bao ZW et al., 2016; Wang DZ et al., 2019b).

Fluid inclusions in pyrites exhibit $^3He/^4He$ ratios of 2.1 Ra to 5.2 Ra for vein ores and 0.3 Ra to 0.8 Ra for disseminated ores (Fig. 10b; Mao JW et al., 2003). The He isotope compositions suggest that 26%–65% mantle-derived helium was added to the fluids responsible for forming the vein ores, while the fluids precipitating the disseminated ores incorporated more crustal-derived helium.

(ii) Material source

The $\delta^{34}S$ values of sulfides range from −13.7‰ to −5.5‰ (Fig. 11a). The negative $\delta^{34}S$ values can be interpreted as biogenic, sedimentary sulfur in origin, or isotope fractionation driven by high oxygen fugacity and boiling of magmatic-derived fluids (Chaussidon M and Lorand JP, 1990; Ohmoto H and Goldhaber MB, 1997). Biogenic or sedimentary sulfur origin could be excluded due to lack of biogenic texture and high $\delta^{34}S$ values (0–4.4‰) for the metamorphic rocks (Wang Y et al., 1990). The existence of sulfur isotope fractionation in these deposits is supported by the coprecipitation of sulfate and sulfides, driven by high oxygen fugacity and ore-forming fluid boiling (Wang DZ et al., 2019b; Zhen SM et al., 2023). Song GR and Zhao ZH (1996) calculated the total S isotopic compositions ($\delta^{34}S$) for the Dongping deposit to be −1‰ to +2‰, similar to those of pyrite in the Shuiquangou syenite ($\delta^{34}S$=+1.8‰ to + 3‰, Nie FJ, 1998; Bao ZW et al., 2016) and rocks of the Archean Sanggan metamorphic complex ($\delta^{34}S$=−0.04‰ to + 4.4‰, Wang Y et al., 1990). Moreover, the Shuiquangou syenite contains magnetite (Zhen SM et al., 2021), indicating high oxygen fugacity of both magma and the resultant hydrothermal fluids. Therefore, the sulfur in ore-forming fluid may be sourced from the Shuiquangou syenites, but a contribution of sulfur from the Archean metamorphic rocks cannot be excluded.

Pb isotopes of different sulfides in the Dongping deposit are stable, with $^{206}Pb/^{204}Pb$, $^{207}Pb/^{204}Pb$ and $^{208}Pb/^{204}Pb$ ranging from 17.587 to 17.639, 15.494 to 15.521 and 37.967 to 37.700, respectively. On the diagrams of $^{207}Pb/^{204}Pb$ *vs.* $^{206}Pb/^{204}Pb$, $^{208}Pb/^{204}Pb$ *vs.* $^{206}Pb/^{204}Pb$ and $^{208}Pb/^{206}Pb$ *vs.* $^{207}Pb/^{206}Pb$, the samples all fall between the lead isotope evolution lines of the orogene and mantle (Figs. 11b–c). Lead isotope of sulfide, disseminated ore, syenitic plutons and the Archean Sanggan metamorphic complex are collinear, indicating a mixing source of Pb for ore-forming processes (Bao ZW et al., 2016). Pb isotopic compositions of ores are similar to that of host syenite, but different from the metamorphic complex of Sanggan Group. Therefore, Pb for mineralization of the Dongping deposit are mainly provided by the Shuiquangou complex, and the strata is not the main source. This is also different from the mixed lead of magmatic rocks and metamorphic rocks, such as Xiaoyingpan and Dabaiyang gold deposits, whose ore body occur in Archean metamorphic rocks (Zhen SM et al., 2021).

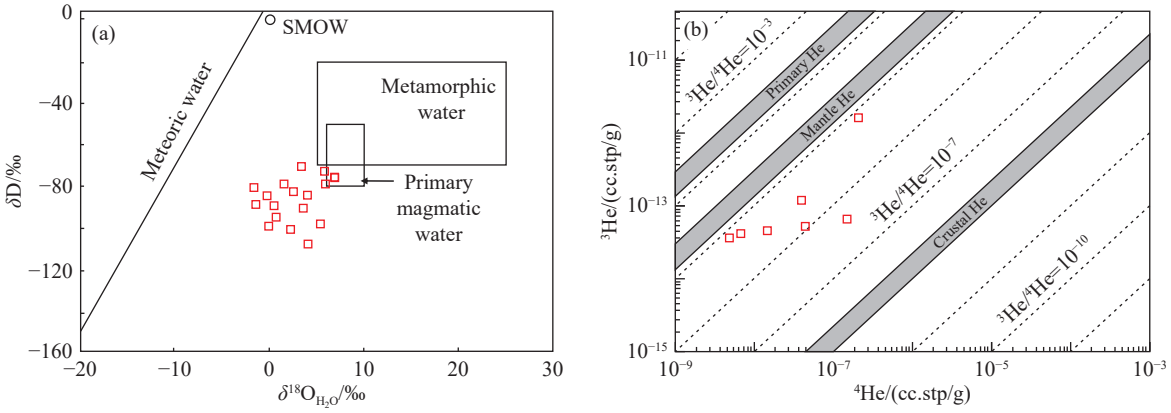

Fig. 10. a–H-O; and b–He isotope compositions of the Dongping gold deposit. δD and $\delta^{18}O_{H2O}$ source from Bao ZW et al. (2016) and Wang DZ et al. (2019b); ^3He and ^4He source from Mao JW et al. (2003).

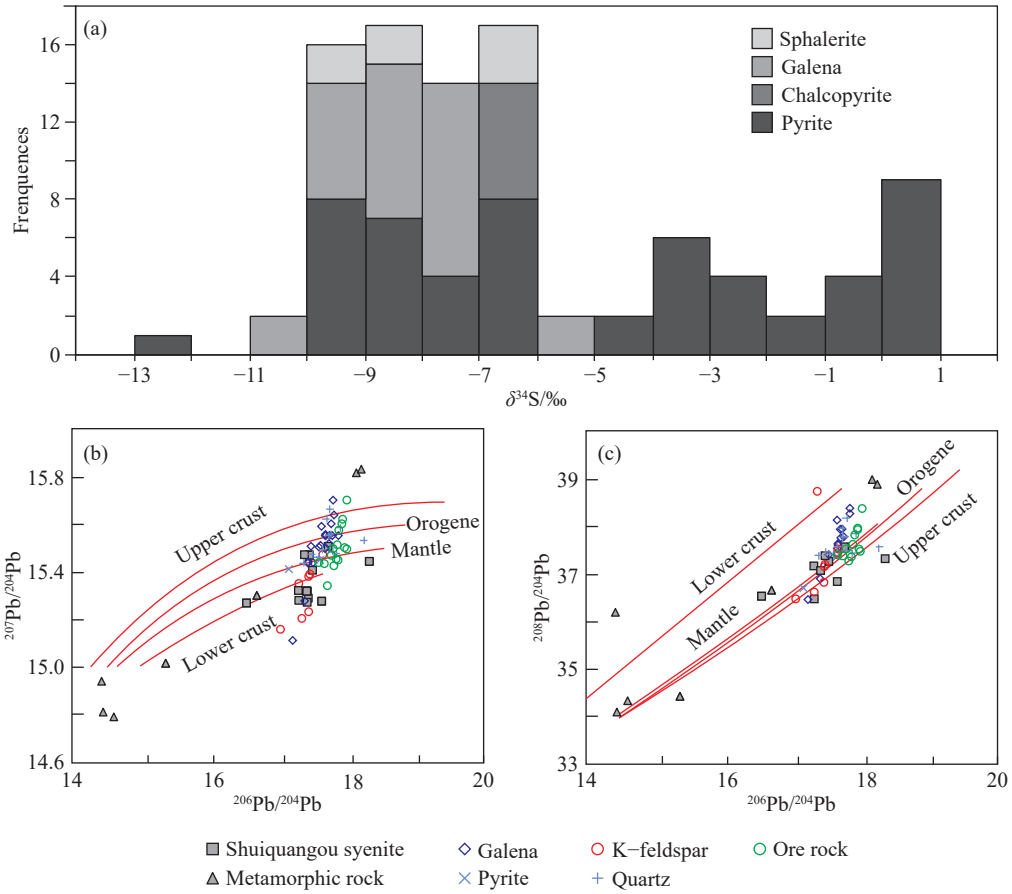

Fig. 11. a–S; and b–c–Pb isotope compositions of the Dongping gold deposit. S isotopes source from Wang Y et al. (1990), Song GR and Zhao ZH (1996), Bao ZW et al. (2016), Wang DZ et al. (2019b), Zhen SM et al. (2021, 2023); Pb isotopes source from Bao ZW et al. (2016).

7.3. Physicochemical conditions for mineralization

The pH value of Stages I and II fluids can be constrained by the K-feldspar-sericite assemblage. The calculated pH is 5.6. According to the salinity and homogenization temperature of fluid inclusions, pH for Stage III is 5.8–5.9 (Liu B and Shen K, 1999). Stage I fluids are constrained to be −27.4 for log f_{O2}, −1.1 for log f_{H2S} and −7.0 for log f_{S2}.

Stage II can be divided into Stage II-1, Stage II-2 and Stage II-3 according to mineral assemblages (Fig. 12). The calculated values of logf_{O2} and logf_{H2S} in stage II-1 were −27.4 to −25.2 and −1.1 to −0.6, respectively. The calculated logf_{S2} value range is −7.0 to −5.2. From stage II-1 to stage II-2, there are no logf_{O2} changes, but logf_{S2} decreases between −9.5 to −7.5, and logf_{Te2} changes between −8.6 to −6.6. The value ranges of logf_{S2} and logf_{Te2} for stage II-3 are −9.5 to −7.2 and −7.6 to −5.3, respectively.

The physicochemical conditions of Stage III cannot be defined because of the lacking of mineral assemblage. Combined with the pH values, the logf_{O2} of Stage III is higher than 36.2.

7.4. Mechanisms of mineral precipitation

Mechanisms of mineral precipitation are dependent on aqueous complexes of metals in fluids. Chloride, bisulfide and hydroxide are the most important ligands for the transport of metals (e.g., Cu, Pb, Zn, Ag and Au) in hydrothermal fluids (Seward TM et al., 2014; Zhong RC et al., 2015). Metal species in fluids are dependent on temperature, redox conditions and availability of ligands (Lukanin OA et al., 2013; Stefánsson A and Sewardb TM, 2003a, 2003b, 2004; Yardley BWD, 2005). Metal precipitations are triggered by boiling, cooling, mixing with other fluids or water-rock interaction (Cooke DR and McPhail DC, 2001; Reed HM and Palandri JL, 2006).

Many minerals precipitated from Stage I to Stage II in the Dongping gold deposit, indicating that the physicochemical conditions of fluid had been changed. Fluid temperatures of Stage I and Stage II had not obviously changed, therefore, cooling is ruled out to be the main mechanism for mineral precipitation. Moreover, Au, Ag, Pb and Cu will not precipitate during cooling process (Cooke DR and McPhail DC, 2001), which is not the case for the Dongping deposit. Fluid boiling will lead to the precipitation of many ore-forming elements, which has been proved to be the key factor of mineral precipitation in many porphyry copper deposits and epithermal deposits (Simmons SF et al., 2005). Fluid boiling could promote volatile release (including H_2, O_2, H_2S and Te_2) and decrease temperature, lead to reduction of HS^- and HTe^- contents in the fluid, and promote deposition of sulfides, native gold and native silver but not tellurides. During boiling, Te will enter the gas phase (Grundler PV et

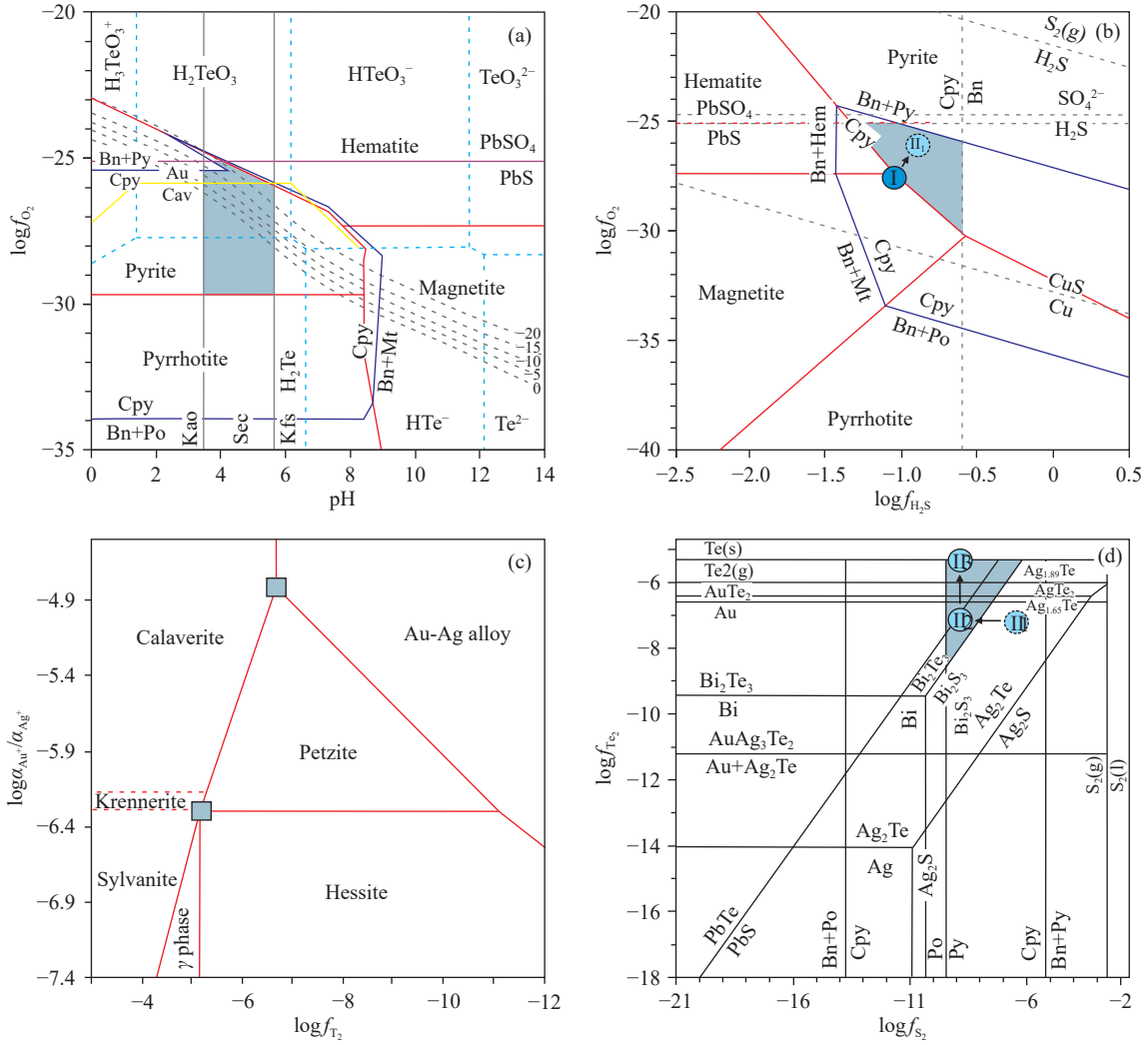

Fig. 12. Physicochemical conditions for different mineralization stages of the Dongping gold deposit (modified from Wang DZ et al., 2019b). The conditions of establishing phase diagram are: $T = 350°C$, $P = 200$ bars, $\alpha_{\Sigma S} = 10^{-2}$, $\alpha_{K+} = 10^{-2}$ and $\alpha_{Te} = 10^{-9}$.From Stage I through Stage II to Stage III, ore-forming fluids of the Dongping deposit show a general trend of increasing oxygen fugacity and decreasing sulfur fugacity, while tellurium fugacity increased in the Stage II-2 and decreased in Stage II-3. This trend is closely related to the processes of mineral precipitation and fluid evolution.

al., 2013). Once the gas phase interacts with the cooling wallrocks, Te in gas phase would be back into the fluids and form droplets, which may result in local saturation of Te in fluid and precipitation of tellurides and native tellurium.

From the above review, it can be seen that there are different mechanisms for mineral precipitation in different stages of mineralization for the Dongping deposit. Sulfide precipitation from Stage I to Stage II may be triggered by fluid boiling, and then precipitation of Pb-Bi telluride mainly resulted from decrement of sulfur fugacity due to sulfide precipitation. Condensation of gas phase containing high concentration of H_2Te leads to precipitation of Te-Au-Ag minerals and native tellurium.

7.5. Metallogenic model

Numerous metallogenic models have been proposed to explain the formation of the Dongping deposit, including the greenstone-type, orogenic-type, remobilization-type, and alkaline intrusion-related type (Bao ZW et al., 2014; Fan GH et al., 2021; Gao S et al., 2015; Hart CJ et al., 2002; Jiang SH and Nie FJ, 1998; Li H et al., 2022; Lu DL et al., 1993; Mao JW et al., 2003; Nie FJ, 1998; Wang ZK et al., 1992; Zhang ZC and Mao JW, 1995). Some researchers have considered the Dongping deposit as a greenstone-type gold deposit due to its host rocks, which include the Shuiquangou complex and the Archean Sanggan metamorphic complex, both of which contain higher gold concentrations compared to the average crust (Liu HT, 1999; Yin JZ and Zhai YS, 1994).

The Dongping gold deposit shares some characteristics with orogenic gold deposits, such as a lack of sulfide, a rich association of tellurium in the ore minerals, a network-like ore structure, and ore-forming fluids characterized by low salinity and high CO_2 content (Hart CJ et al., 2002). Orogenic gold deposits are typically associated with greenschist facies metamorphic rocks, and the ore-forming age of the Dongping deposit is much younger than the metamorphic age of the Archean Sanggan complex. While the Archean Sanggan rocks lost most of their volatiles during metamorphism, which

might not have provided sufficient metamorphic fluids for gold mineralization (Bao ZW et al., 2016), it is argued that the Devonian Shuiquangou syenite may have played a similar role to that of the metamorphic rocks within the Sanggan Group, serving as a potential source of gold for the mineralization in the Zhangjiakou district (Zhen SM et al., 2021). The regional distribution of gold mineralization, controlled by the northeast-oriented Yanshanian magmatic zone and the presence of east-west wall rocks, including the Devonian syenite and the Archean metamorphic rocks, further supports this hypothesis (Zhen SM et al., 2021).

The isotope compositions and formation ages of the Dongping deposit provide evidence suggesting that the Shuiquangou syenite may have been one of the primary source of metals in the gold mineralization process. U-Pb ages of hydrothermal zircons and garnet indicate that the deposit experienced hydrothermal overprints during the Late Jurassic-Early Cretaceous (Bao ZW et al., 2014; Fan GH et al., 2021; Li CM et al., 2010a, 2010b). Li H et al. (2022) proposed that the Dongping gold deposit resulted from two stages of mineralization. The first stage occurred during the Devonian period (ca 380 Ma) and is linked to the intrusion of the Shuiquangou syenite. The second stage of mineralization is associated with the emplacement of the Cretaceous (ca 140 Ma) Shangshuiquan granite, which formed due to the subduction of the Paleo-Pacific Plate beneath the North China Craton. During the Late Jurassic to Early Cretaceous, fluids originating from granitic magmatism mixed with meteoric waters, leading to the remobilization of the initial gold mineralization and a second phase of enrichment.

The Dongping gold deposit likely formed by multiple mineralization events. During the Devonian period, the subduction of the Paleo-Asian Ocean beneath the North China Craton resulted in the partial melting of the lithospheric mantle, leading to the formation of widespread alkaline rocks (Fig. 13a). As the magmatic-hydrothermal fluid interacted with the metamorphic rocks of the Sanggan Group, the physicochemical conditions of the ore-forming fluid underwent significant changes, leading to the precipitation of early mineralization. During the migration and emplacement of magma, substantial fluid exsolution and degassing occurred. The fluid and gas phases migrated towards the surface through faults and fractures, continuously scavenging ore-forming materials from the surrounding rock and precipitating minerals either at the early mineralization site or other favorable locations. During the Jurassic-Cretaceous

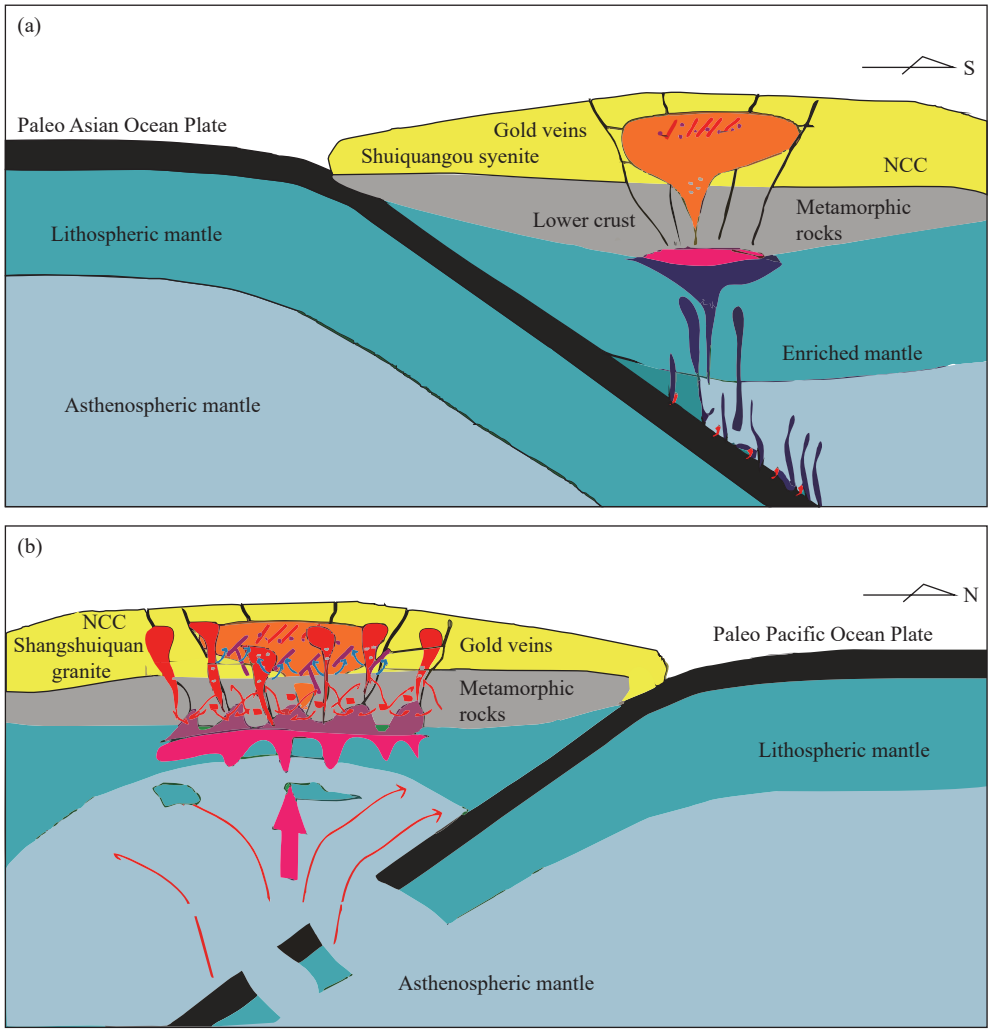

Fig. 13. Block diagram illustrating the genesis of the Dongping-type deposit (modified from Li H et al., 2018).

period, the Paleo-Asian Ocean closed, and the Paleo-Pacific plate subducted beneath the Asian continent, resulting in extensive magmatic activities in the Zhangjiakou district (Fig. 13b). The highly evolved Shangshuiquan granite released fluorine-rich fluids, which ascended along the early mineralization site, continuously collecting gold from the previously mineralized rocks. This process concentrated gold, ultimately leading to the formation of the Dongping gold deposit.

7.6. Integrated prospecting model

Based on the metallogenic models and a combination with regional mineral geological survey, the integrated geology-gravity-magnetic-geochemistry prospecting model have been constructed for gold deposits in the study area (Liang HF, 1995; Zou GH, 1996, Zhen SM et al., 2019).

Geological prospecting indicator: The host rock of the orebody is the Shuiquangou complex and the Archean Sanggan metamorphic complex. The ore-controlling structure is a composite part of NNE-EW-SN-SW, NE-NWW-NW, NNE-NW trending structures. The favorable ore bearing structures are NNE and NW trending faults. Within the mining field, NNE trending faults are conducive to the formation of ore deposits, and the favorable areas for mineralization are the areas where NNE leftward and NW rightward echelon veins occur. The activity of NEE trending faults is poor, which is not conducive to mineralization. The signs of alteration are silicification, potassic alteration, sericitization, and pyrite mineralization. The age of the ore-forming igneous rocks is the Yanshanian.

Gravity-aeromagnetic anomalies: On the three 1∶50000 gravity maps of Chongli, Zhaochuan and Changyukou, the Bouguer anomaly values range from -157×10^{-5} m/s^2 to -104×10^{-5} m/s^2, with a field variation amplitude of 53×10^{-5} m/s^2. The overall gravity field exhibits a gravity anomaly feature of high in the SW and low in the NE. The distribution direction of contour lines is mainly NW, followed by NS and NE directions. The Dongping gold mine is located in the north of the NW contour line. On the three 1∶50000 aeromagnetic anomaly map, the range of aeromagnetic anomalies is from −743 to 3809 nT, similar to those of gravity Bouguer anomalies. Most areas exhibit characteristics of "high magnetism-high gravity" or "low magnetism-low gravity". The high-value zones of aeromagnetic and gravity match with the uplifted areas of the exposed high-density old strata. The low gravity zone is spatially associated with by low-density blocks such as the Quaternary system. The high-value areas of aeromagnetic anomalies fixed with metamorphic rocks and intrusive rocks. Multiple gold deposits were discovered in this area, mostly with distribution on the edge of low gravity or low gravity gradient zones, as well as the edges of high magnetic anomalies.

Geochemistry anomalies: The 1∶50000 geochemical stream sediment survey shows that the contents of Au, Ag, Bi, Cd, Cr, Co, Cu, Mo, Ni, Pb, W, Zn, Te, and Se elements in the Archean Sanggan metamorphic complex are relatively high. The content and coefficient of variation of Au elements in the Shuiquangou complex are high, and the number of variation series of elements, such as Ag, Bi, Pb Te, and Se, is large. The correlation analysis of geochemical stream sediment shows that there is a weak correction between Au and Mo, Ag, and Te, and a strong correction between Ag and Se, Te, Pb, Cu, and Bi. In the mining field and its surrounding areas, Au, Ag, Hg, As, and Sb are characterized by high background values. These elements are concentrated and distributed along anticlines and magmatic rock zones. It has been found that the Au element anomaly area in the gold deposit is large, with clear concentration zoning. Au, Ag, Pb, Bi, Te, Mo, Cd, As, Hg, and Sb have a unified concentration center, and the anomaly fit is good. Dongping gold deposit is located at the intersection of NE to EW Au high background, while Xiaoyingpan and Dabaiyang gold deposits are located at the intersection of NE to NW gold high background. The geochemical erosion degree mapping, using (As+Sb+Hg)/(W+Sn+Mo), shows that the discovered gold deposit experienced a moderate degree of erosion.

8. Conclusions

The key findings of this study are:

(i) The Dongping gold deposit is the largest alkaline intrusion-hosted gold deposit in China. It contains more than 100 t gold.

(ii) Sulfide precipitation from Stage I to Stage II may be triggered by fluid boiling, and then precipitation of Pb-Bi telluride mainly resulted from decrement of sulfur fugacity. Condensation of gas phase containing high concentration of H_2Te leads to precipitation of Te-Au-Ag minerals and native tellurium.

(iii) The early mineralization at Dongping is genetically associated with the Devonian Shuiquangou alkaline complex and overprinted by hydrothermal activities of Late Jurassic to Early Cretaceous.

(iv) As a large-sized gold deposit, the formation, preservation and discovery of the Dongping deposit provide an important indication for exploration of ancient porphyry-epithermal deposits in the north margin of the North China Craton.

CRediT authorship contribution statement

Shi-Min Zhen and Da-Zhao Wang conceived of the present idea, took the lead in writing the manuscript and developed theory. Zhong-Jian Zha, Hai-Jun Bai and Jiang Wang contributed to the interpretation of the results and carried out the experiment.

Declaration of competing interest

The authors declare no conflicts of interest.

Acknowledgment

This study was financially supported by the project of the

China Geological Survey (DD20230292, DD20242591). The manuscript has benefited from valuable advice from Prof. Tian-Zhu Ye and Zi-Hao Hao.

References

Bao ZW, Li CJ, Zhao ZH. 2016. Metallogeny of the syenite-related Dongping gold deposit in the northern part of the North China Craton: A review and synthesis. Ore Geology Reviews, 73, 198–210. doi: 10.1016/j.oregeorev.2015.04.002.

Bao ZW, Sun WD, Li CJ, Zhao ZH. 2014. U-Pb dating of hydrothermal zircon from the Dongping gold deposit in North China: Constraints on the mineralization processes. Ore Geology Reviews, 61, 107–119. doi: 10.1016/j.oregeorev.2014.02.006.

Bindi L, Arakcheeva A, Chapuis G. 2009. The role of silver on the stabilization of the incommensurately modulated structure in calaverite, $AuTe_2$. American Mineralogist, 94, 728–736. doi: 10.2138/am.2009.3159.

Chaussidon M, Lorand JP. 1990. Sulphur isotope composition of orogenic spinel lherzolite massifs from Ariege (North-Eastern Pyrenees, France): An ion microprobe study. Geochimica et Cosmochimica Acta, 54, 2835–2846. doi: 10.1016/0016-7037(90)90018-G.

Cisse M, Lu X, Algeo TJ, Cao XF, Li H, Wei M, Yuan Q, Chen M. 2017. Geochronology and geochemical characteristics of the Dongping ore-bearing granite, North China: Sources and implications for its tectonic setting. Ore Geology Reviews, 89, 1091–1106. doi: 10.1016/j.oregeorev.2016.07.006.

Cook NJ, Ciobanu CL. 2004. Bismuth tellurides and sulphosalts from the Larga hydrothermal system, Metaliferi Mts, Romania: Paragenesis and genetic significance. Mineralogical Magazine, 68, 301–321. doi: 10.1180/0026461046820188.

Cook NJ, Ciobanu CL, Mao JW. 2009. Textural control on gold distribution in As-free pyrite from the Dongping, Huangtuliang and Hougou gold deposits, North China Craton (Hebei Province, China). Chemical Geology, 264, 101–121. doi: 10.1016/j.chemgeo.2009.02.020.

Cooke DR, McPhail DC. 2001. Epithermal Au-Ag-Te mineralization, Acupan, Baguio district, Philippines: Numerical simulations of mineral deposition. Economic Geology, 96, 109–131. doi: 10.2113/gsecongeo.96.1.109.

Cui SQ, Li RJ, Wu ZH, Yi MC, Shen SM, Yi HR, Ma YS. 2002. Mesozoic and Cenozoic intracontinental orogeny of the Yanshan region, China. Beijing, Geological Publishing House, 1–100 (in Chinese).

Deng J, Wang QF. 2016. Gold mineralization in China: Metallogenic provinces, deposit types and tectonic framework. Gondwana Research, 36, 219–274. doi: 10.1016/j.gr.2015.10.003.

Fan GH, Li JW, Deng XD, Gao WS, Li SY. 2021. Age and origin of the Dongping Au-Te deposit in the North China Craton Revisited: Evidence from paragenesis, geochemistry, and in situ U-Pb geochronology of garnet. Economic Geology, 116(4), 963–985. doi: 10.5382/econgeo.4810.

Fan GH, Li JW, Valley JW, Scicchitano MR, Brown PE, Yang JH, Robinson PT, Deng XD, Wu YF, Li ZK, Gao WS, Li SY, Zhao SR. 2022. Garnet secondary ion mass spectrometry oxygen isotopes reveal crucial roles of pulsed magmatic fluid and its mixing with meteoric water in lode gold genesis. Proceedings of the National Academy of Sciences, 119(18), 1–8. doi: 10.1073/pnas.2116380119.

Fan HR, Xie YH, Zhai MG. 2001. Ore-forming fluids in the Dongping gold deposit, northwestern Hebei Province. Science in China Series D:Earth Sciences, 44(8), 748–757. doi: 10.1007/BF02907204.

Fu C, Dang ZC, Li JJ, Zhou SM, Ni ZP, Peng Y, Song LJ, Zhang T, Hou ZG. 2022. Regional metallogeny and resource potential of gold deposits in North China. Geology in China, 49(4), 1179–1197 (in Chinese with English abstract). doi: 10.12029/gc20220410.

Gao S, Xu H, Li SR, Santosh M, Zhang DS, Yang LJ, Quan SL. 2017. Hydrothermal alteration and ore-forming fluids associated with gold-tellurium mineralization in the Dongping gold deposit, China. Ore Geology Reviews, 80, 166–184. doi: 10.1016/j.oregeorev.2016.06.023.

Gao S, Xu H, Zhang DS, Shao HN, Quan SL. 2015. Ore petrography and chemistry of the tellurides from the Dongping gold deposit, Hebei Province, China. Ore Geology Reviews, 64, 23–34. doi: 10.1016/j.oregeorev.2014.06.010.

Grundler PV, Brugger J, Etschmann BE, Helm L, Liu WH, Spry PG, Tian Y, Testemale D, Pring A. 2013. Speciation of aqueous tellurium(IV) in hydrothermal solutions and vapors, and the role of oxidized tellurium species in Te transport and gold deposition. Geochimica et Cosmochimica Acta, 120, 298–325. doi: 10.1016/j.gca.2013.06.009.

Hart CJ, Goldfarb RJ, Qiu YM, Snee L, Miller LD, Miller ML. 2002. Gold deposits of the northern margin of the North China Craton: Multiple late Paleozoic–Mesozoic mineralizing events. Mineralium Deposita, 37, 326–351. doi: 10.1007/s00126-001-0239-2.

Jiang N, Liu YS, Zhou WG, Yang JH, Zhang SQ. 2007. Derivation of Mesozoic adakitic magmas from ancient lower crust in the North China Craton. Geochimica et Cosmochimica Acta, 71, 2591–2608. doi: 10.1016/j.gca.2007.02.018.

Jiang N, Zhang SQ, Zhou WG, Liu YS. 2009. Origin of a Mesozoic granite with A-type characteristics from the North China Craton: Highly fractionated from I-type magmas?. Contributions to Mineralogy and Petrology, 158, 113–130. doi: 10.1007/S00410-008-0373-2.

Jiang N. 2005. Petrology and geochemistry of the Shuiquangou syenitic complex, northern margin of the North China Craton. Journal of the Geological Society, 162, 203–215. doi: 10.1144/0016-764903-144.

Jiang SH, Nie FJ. 1998. A comparison study on geological and geochemical features and ore genesis of the Xiaoyingpan and Dongping gold deposits, Hebei. Gold Geology, 4(4), 12–24 (in Chinese with English abstract).

Jiang SH, Nie FJ. 2000. $^{40}Ar/^{39}Ar$ geochronology of the Shuiquangou alkaline complex and related gold deposits, Northwestern Hebei, China. Geological Review, 46(6), 621–627 (in Chinese with English abstract). doi: 10.16509/j.georeview.2000.06.012.

Li CJ, Bao ZW, Zhao ZH, Qiao YL. 2012. Zircon U-Pb age and Hf isotopic compositions of the granitic gneisses from the Sanggan complex in the Zhangjiakouk area: Constraints on the early evolution of North China Craton. Acta Petrologica Sinica, 28(4), 1057–1072 (in Chinese wirh English abstract).

Li CM, Deng JF, Chen LH, Su SG, Li HM, Hu SL, Liu XM. 2010a. Two periods of zircon from Dongping gold deposit in Zhangjiakou-Xuanhua area, northern margin of North China: Constraints on metallogenic chronology. Mineral Deposits, 29(2), 265–275 (in Chinese with English abstract). doi: 10.16111/j.0258-7106.2010.02.008.

Li CM, Deng JF, Su SG, Li HM, Liu XM. 2010b. Two stage zircon U-Pb ages of the potash altered rock in the Dongping gold deposit, Hebei Province, and their geological implications. Acta Geoscientica Sinica, 31(6), 843–852 (in Chinese with English abstract).

Li H, Li JW, Algeo TJ, Wu JH, Cisse M. 2018. Zircon indicators of fluid sources and ore genesis in a multi-stage hydrothermal system: The Dongping Au deposit in North China. Lithos, 314–315, 463–478. doi: 10.1016/j.lithos.2018.06.025.

Li H, Zhu DP, Algeo TJ, Li M, Jiang WC, Chen SF, Elatikpo SM. 2022. Pyrite trace element and S-Pb isotopic evidence for contrasting sources of metals and ligands during superimposed hydrothermal

events in the Dongping gold deposit, North China. Mineralium Deposita, 58(2), 337–358. doi: 10.1007/s00126-022-01128-w.

Li HY, Zhang ZY, Li P, Xing GH. 2000. Structural analysis and genesis of gold deposit in the Dongping. Geology and Prospecting, 36(5), 36–38 (in Chinese with English abstract).

Li JL, Makovicky E. 2001. New studies on mustard gold from the Dongping Mines, Hebei Province, China: The tellurian, plumbian, manganoan and mixed varieties. Neues Jahrbuch Fur Mineralogie-Abhandlungen, 176, 269–297. doi: 10.1127/njma/176/2001/269.

Li SZ. 1999. Control of echelon vein on mineralization and its indication to prospecting. Geology and Prospecting, 35(6), 15–19 (in Chinese with English abstract).

Li SZ, Qi GC. 2000. Geological characteristics and structural ore-controlling role of the Dongping gold deposit, Hebei Province. Acta Geosicientia Sinica, 21(1), 44–51 (in Chinese with English abstract).

Li, CJ, Bao ZW. 2012. Geochemical characteristics and geodynamic implications of the Early Cretaceous magmatisms in Zhangjiakou region, northwest Hebei Province, China. Geochimica, 41(4), 343–358 (in Chinese with English abstract). doi: 10.19700/j.0379-1726.2012.04.004.

Liang HF. 1995. A preliminary study of “three-stages & two-series” prospecting model in Dongping deposit. Gold Geology, 1(1), 42–45 (in Chinese with English abstract).

Liu B, Shen K. 1999. Thermo-dynamics of fluid inclusions. Beijing, Geological Publishing House, 16–180 (in Chinese).

Liu HT. 1999. Analysis of ore-controlling factors of Huangtuliang gold deposit, northwest Hebei Province. Journal of Precious Metallic Geology, 8(4), 209–216 (in Chinese with English abstract).

Lu DL, Luo XQ, Wang JJ, Zhang SH, Zheng BY. 1993. The metallogenic epoch of the Dongping gold deposit. Mineral Deposits 12(2), 182–188 (in Chinese with English abstract).

Lukanin OA, Ryzhenko BN, Kurovskaya NA. 2013. Zn and Pb solubility and speciation in aqueous chloride fluids at T-P parameters corresponding to granitoid magma degassing and crystallization. Geochemistry International, 51(10), 802–830. doi: 10.1134/S0016702913090048.

Mao JW, Li YQ, Goldfarb R, He Y, Zaw K. 2003. Fluid inclusion and noble gas studies of the Dongping gold deposit, Hebei Province, China: A mantle connection for mineralization? Economic Geology, 98(3), 517–534. doi: 10.2113/gsecongeo.98.3.517.

Miao LC, Qiu YM, McNaughton N, Luo ZK, Groves D, Zhai YS, Fan WM, Zhai MG, Guan K. 2002. SHRIMP U-Pb zircon geochronology of granitoids from Dongping area, Hebei Province, China: constraints on tectonic evolution and geodynamic setting for gold metallogeny. Ore Geology Reviews, 19, 187–204. doi: 10.1016/S0169-1368(01)00041-5.

Nie FJ. 1998. Geology and origin of the Dongping alkalic-type gold deposit, Northern Hebei province, People’s Republic of China. Resource Geology, 48(3), 139–158. doi: 10.1111/j.1751-3928.1998.tb00013.x.

Ohmoto H, Goldhaber MB. 1997. Sulfur and carbon isotopes. In: Barnes HL, (Ed.), Geochemistry of Hydrothermal Ore Deposits. Wiley, New York, 517–612.

Pals DW, Spry PG. 2003. Telluride mineralogy of the low-sulfidation epithermal Emperor gold deposit, Vatukoula, Fiji. Mineralogy and Petrology, 79, 285–307. doi: 10.1007/s00710-003-0013-5.

Reed MH, Palandri JL. 2006. Sulfide mineral precipitation from hydrothermal fluids. Reviews in Mineralogy and Geochemistry 61, 609–631. doi: 10.2138/rmg.2006.61.11.

Roedder E. 1984. Fluid Inclusions. In: Ribbe, P. H. (Ed.), Reviews in Mineralogy. Mineralogical Society of America, Washington, D. C., 644.

Scherbarth NL, Spry PG. 2006. Mineralogical, petrological, stable isotope, and fluid inclusion characteristics of the Tuvatu gold-silver telluride deposit, Fiji: comparisons with the emperor deposit. Economic Geology, 101, 135–158. doi: 10.2113/gsecongeo.101.1.135.

Seward TM, Williams-Jones AE, Migdisov AA. 2014. The chemistry of metal transport and deposition by ore-forming hydrothermal fluids. In: Holland HD, Turekian K K, (Eds.), Treatise on Geochemistry 2nd Edition. Elsevier Science, UK, 29–57. doi: 10.1016/B978-0-08-095975-7.01102-5.

Simmons SF, White NC, John DA. 2005. Geological Characteristics of Epithermal Precious and Base Metal Deposits. Economic Geology, 100, 485–522. doi: 10.5382/AV100.16.

Song GR, Zhao ZH. 1996. Geology of Dongping alkaline complex-hosted gold deposit in Hebei Province. Beijing, Seismological Press, 185–212 (in Chinese).

Spry PG, Foster F, Truckle JS. 1997. The mineralogy of the golden sunlight gold-silver telluride deposit, Whitehall, Montana, U. S. A. Mineralogy and Petrology, 59, 143–164. doi: 10.1007/BF01161857.

Stefánsson A, Seward TM. 2003a. Experimental determination of the stability and stoichiometry of sulphide complexes of silver(I) in hydrothermal solutions to 400°C. Geochimica et Cosmochimica Acta, 67, 1395–1413. doi: 10.1016/S0016-7037(02)01093-1.

Stefánsson A, Seward TM. 2003b. Stability of chloridogold(I) complexes in aqueous solutions from 300 to 600°C and from 500 to 1800 bar. Geochimica et Cosmochimica Acta, 67, 4559–4576. doi: 10.1016/S0016-7037(03)00391-0.

Stefánsson A, Seward TM. 2004. Gold(I) complexing in aqueous sulphide solutions to 500°C at 500 bar. Geochimica et Cosmochimica Acta, 68, 4121–4143. doi: 10.1016/j.gca.2004.04.006.

Tian W, Chen B, Liu Chaoqun, Zhang Huafeng. 2007. Zircon U-Pb age and Hf isotopic composition of the Xiaozhangjiakou ultramafic pluton in northern Hebei. Acta Petrologica Sinica, 23(3), 583–590 (in Chinese with English abstract).

Villa IM, Hanchar JM. 2013. K-feldspar hygrochronology. Geochimica et Cosmochimica Acta, 101, 24–33. doi: 10.1016/j.gca.2012.09.047.

Wang DZ, Liu JJ, Carranza EJM, Zhai DG, Wang YH, Zhen SM, Wang J, Wang JP, Liu ZJ, Zhang FF. 2019a. Formation and evolution of snowball quartz phenocrysts in the Dongping porphyritic granite, Hebei Province, China: Insights from fluid inclusions, cathodoluminescence, trace elements, and crystal size distribution study. Lithos, 340–341, 239–254. doi:10.1016/j.lithos.2019.05.018.

Wang DZ, Liu JJ, Zhai DG, Carranza EJM, Wang YH, Zhen SM, Wang J, Wang JP, Liu ZJ, Zhang FF. 2019b. Mineral paragenesis and ore‐forming processes of the Dongping gold deposit, Hebei Province, China. Resource Geology, 69, 287–313. doi: 10.1111/rge.12202.

Wang DZ, Liu JJ, Zhai DG, de Fourestier J, Wang YH, Zhen SM, Wang JP, Liu ZJ, Zhang FF. 2020a. Textures and formation of microporous gold in the Dongping gold deposit, Hebei Province, China. Ore Geology Reviews, 120, 103437. doi: 10.1016/j.oregeorev.2020.103437.

Wang DZ, Liu JJ, Zhai DG, Zhen SM, Wang J, Yang XA. 2019c. New discovery of molybdenite in the Dongping gold deposit, Hebei province, China and its Re-Os geochronological implication. Acta Geologica Sinica (English Edition), 93, 769–770. doi: 10.1111/1755-6724.13841.

Wang DZ, Liu JJ, Zhai DG, Zhen SM, Wang J. 2020b. Study on molybdenite Re-Os and zircon U-Pb ages of the Dongping tellurium-gold deposit, Hebei Province. Earth Science Frontiers, 27(2), 405–419 (in Chinese with English abstract). doi: 10.13745/j.esf.sf.2020.3.29.

Wang DZ, Zhen SM, Liu JJ, John M, Carranza E, Wang J, Zha ZJ, Li Y, Bai HJ. 2021. Mineral paragenesis and hydrothermal evolution of the Dabaiyang tellurium-gold deposit, Hebei Province, China: Constraints from fluid inclusions, H-O-He-Ar isotopes, and physicochemical conditions. Ore Geology Reviews, 130, 103904.

doi: 10.1016/j.oregeorev.2020.103904.

Wang Y, Jiang XM, Wang ZK. 1990. Characteristics of lead and sulfur isotope of the gold deposits in Zhangjiakou Xuanhua area, Hebei Province. Contributions to Geology and Mineral Resources Research, 5(2), 66–75 (in Chinese with English abstract).

Wang ZK, Jiang XM, Wang Y, Shang MY. 1992. A comparative analysis on geological-geochemical features of the Xiaoyingpan and Dongping gold deposits, Hebei. Geology and Exploration, 7, 14–20 (in Chinese with English abstract).

Wei H, Xu JH, Zhang GR, Cheng XH, Chu HX, Bian CJ, Zhang ZY. 2018. Hydrothermal metasomatism and gold mineralization of porphyritic granite in the Dongping Deposit, North Hebei, China: Evidence from Zircon Dating. Minerals, 8(9), 363. doi: 10.3390/min8090363.

Xiao CH, Chen ZL, Yao XF, Liu XC, Liu JM. 2023. The control of deformation partitioning on gold mineralization in the Qingchengzi district, Liaodong Peninsula, northeastern China. Journal of Asian Earth Sciences, 242, 105517. doi: 10.1016/j.jseaes.2022.105517.

Xiao CH, Liu XC, Zhao Y, Zhang Q, Chen ZL. 2020. Structural controls and Re-Os dating of molybdenite of Wulong gold deposit, NE China. Earth Science, 45(11), 3982–3997 (in Chinese with English abstract). doi: 10.3799/dqkx.2020.217.

Yang JH, Wu FY, Shao JA, Xie LW, Liu XM. 2006. In-Situ U-Pb dating and Hf isotopic analyses of zircons from volcanic rocks of the Houcheng and Zhangjiakou Formations in the Zhang-Xuan area, Northeast China. Earth Science-Journal of China University of Geosciences, 31, 71–80.

Yang XA, Wu J, Coulson IM, Zhang J, Lai X, Zhang Y, Xu D, Liu J, Li G, Li H. 2019. Discovery of concealed ore-bodies at the Dongping gold deposit, northern China, revealed by the study of ore-controlling structures. Ore Geology Reviews, 103216. doi: 10.1016/j.oregeorev.2019.103216.

Yardley BWD. 2005. Metal concentrations in crustal fluids and their relationship to ore formation. Economic Geology, 100, 613–632. doi: 10.2113/GSECONGEO.100.4.613.

Yin JZ, Zhai YS. 1994. On the metallogenic series of gold deposits in Zhangjiakou-Xuanhua region, Hebei. Journal of Guilin College of Geology, 14(4), 360–369 (in Chinese with English abstract).

Zeng QD, Wang Y, Yang J, Guo Y, Yu B, Zhou L, Qiu H. 2020. Spatial–temporal distribution and tectonic setting of gold deposits in the northern margin gold belt of the North China Craton. International Geology Review, 63, 1–32. doi: 10.1080/00206814.2020.1737839.

Zhai MG, Santosh M. 2013. Metallogeny of the North China Craton: Link with secular changes in the evolving Earth. Gondwana Research, 24, 275–297. doi: 10.1016/J.GR.2013.02.007.

Zhai MG. 2019. Tectonic evolution of the North China Craton. Journal of Geomechanics 25(5), 722–745 (in Chinese with English abstract). doi:10.12090/j.issn.1006-6616.2019.25.05.063.

Zhang HF. 2007. Temporal and spatial distribution of Mesozoic mafic magmatism in the North China Craton and implications for secular lithospheric evolution. Geological Society, London, Special Publications, 280, 35–54. doi: 10.1144/SP280.2.

Zhang PH, Zhao ZH, Zhu JC, Zhang WL, Bao ZW, Zhang YH. 2002. Tellurides of gold and silver and their capacity of carrying gold in ores from the Dongping-type gold deposits, Hebei Province, China. Acta Mineralogica Sinica, 22(4), 321–329 (in Chinese with English abstract).

Zhang ZC, Mao JW. 1995. Geology and geochemistry of the Dongping gold telluride deposit, Heibei Province, North China. International Geology Review, 37, 1094–1108. doi: 10.1080/00206819509465441.

Zhao GC, Zhai MG. 2013. Lithotectonic elements of Precambrian basement in the North China Craton: Review and tectonic implications. Gondwana Research, 23, 1207–1240. doi: 10.1016/J.GR.2012.08.016.

Zhen SM, Bai HJ, Jia RY, Yao Lei, Zhang ZH, Chen H, Tao W. 2019. Achievement report on the prospecting prediction of Xuanhua-Fengning mining area, Hebei Province. China Geological Survey, 178–237 (in Chinese).

Zhen SM, Wang DZ, Bai HJ, Jia RY, Wang J, Zha ZJ, Li Y, Miao JP. 2021. The Paleozoic-Mesozoic magmatic-tectonic activities and their geological implications in the Zhangjiakou-Xuanhua district, northern margin of the North China Craton. Acta Petrologica Sinica, 37, 1619–1652. doi: 10.18654/1000-0569/2021.06.01.

Zhen SM, Zha ZJ, Wang DZ, Liu JJ, Pang ZS, Cheng ZZ, Xue JL, Wang J, Bai HJ, Li Y, Chen C. 2023. Characteristics of ore-forming fluids of the Zhongshangou gold deposit, Zhangjiakou-Xuanhua area, Hebei Province, and its limitation on the intrusive rock related telluride-gold deposits. Geology in China, 50(2), 605–621 (in Chinese with English abstract). doi: 10.12029/gc20190927002.

Zheng YD, Song GX, Li GH, Zhang C. 1990. Structural analysis of Dongping gold-bearing quarz vein system in Chongli County, Hebei Province. Contributions To Geology and Mineral Resources Research, 5(2), 20–28 (in Chinese with English abstract).

Zhong RC, Brugger J, Chen YJ, Li WB. 2015. Contrasting regimes of Cu, Zn and Pb transport in ore-forming hydrothermal fluids. Chemical Geology, 395, 154–164. doi: 10.1016/J.CHEMGEO.2014.12.008.

Zou GH, Ouyang ZQ, Li H. 1996. Exploration models for major types of gold deposits in China. Beijing, Geological Publishing House, 108–164 (in Chinese).